Spectral Efficiency of MIMO Ad Hoc Networks with Partial Channel State Information

by

Niranjan Thontadarya

A Thesis Presented in Partial Fulfillment
of the Requirement for the Degree
Master of Science

Approved July 2014 by the
Graduate Supervisory Committee:

Daniel Bliss, Chair
Visar Berisha
Lei Ying

ARIZONA STATE UNIVERSITY

August 2014

ABSTRACT

As the number of devices with wireless capabilities and the proximity of these devices to each other increases, better ways to handle the interference they cause need to be explored. Also important is for these devices to keep up with the demand for data rates while not compromising on industry established expectations of power consumption and mobility. Current methods of distributing the spectrum among all participants are expected to not cope with the demand in a very near future. In this thesis, the effect of employing sophisticated multiple-input, multiple-output (MIMO) systems in this regard is explored. The efficacy of systems which can make intelligent decisions on the transmission mode usage and power allocation to these modes becomes relevant in the current scenario, where the need for performance far exceeds the cost expendable on hardware. The effect of adding multiple antennas at either ends will be examined, the capacity of such systems and of networks comprised of many such participants will be evaluated. Methods of simulating said networks, and ways to achieve better performance by making intelligent transmission decisions will be proposed. Finally, a way of access control closer to the physical layer (a 'statistical MAC') and a possible metric to be used for such a MAC is suggested.

ACKNOWLEDGMENTS

On this single most important page of my thesis, I would like to extend my gratitude towards

- My advisor Dr. Daniel W Bliss for his guidance and insight, which were invaluable towards the completion of this work and will inspire all my future endeavors.

- My family for their continuous support and love, which give me incessant motivation in all that I do.

- My buddies for their questionable judgment in making friends, which gave me affection far greater than what I deserve.

TABLE OF CONTENTS

CHAPTER Page

LIST OF TABLES

LIST OF FIGURES

Chapter 1

INTRODUCTION

1.1 Background

The booming use of wireless devices and the remarkable increase in the up-time of users has been challenging electrical engineers for the past decade. As our counterparts in device engineering strive to increase the area efficiency of chips, we, as signal processing and telecommunications engineers, look to increase the spectral efficiency of transmission.

The Edholm's Law of Bandwidth, which is a new proposition that draws parallels between the Moore's Law and the growth in data rate requirements with time, predicts a doubling of this range once every 18 months [4]. Convincingly, in the early 80s, a rate of 1kb/s was deemed acceptable but in twenty years (an expected thousand-fold increase), it grew to 1Mb/s. Traditional systems which have single-input, single-output antennas (SISO) can increase the transmit power or bandwidth to get higher data rates but these options have become largely unattractive because of the said limitation in bandwidth and the need to conserve power for computation in smart devices.

Multiple antennas at the transmit side have been used in transmit beam-forming techniques to get better directionality. Also, multiple antennas at the receive side have been used to obtain diversity by smartly combining the received signals to get better error performance ('link quality') and increase the range. When both the transmit and the receive sides use more than one antenna, a 'capacity multiplicative' effect is seen, where the peak data rate of transmission is increased by many times.

Such a system is referred to as a multiple-input, multiple-output or MIMO system. We will explore the techniques involved in realizing a MIMO system in the second chapter.

MIMO is spoken of as a technology different from phased arrays, in the sense that in MIMO, the multi-path scattering is sufficiently complicated that independent channel gains between any transmitting and receiving antennas is expected. Although at the time of inception, MIMO was seen as an extension of smart antenna systems [5], the technology has advanced enough to merit its own branch in modern telecommunications. Beamforming is a method used in phased array antenna systems to provide directionality to the radiation but offered no improvement in data rate. MIMO supports adaptive beamforming as well as the use of spatial multiplexing (division of data stream and parallel transmission) and spatial diversity (repeated message streams on separate paths) [6]. These techniques are explained in better detail later in this literature.

The biggest advantage of employing MIMO is the increase in the degrees of freedom. On the other hand, the penalty in MIMO technologies happen to be an increase in computation and hardware, which are far less important considerations compared to the need for spectrum [5]. The improvement in the information theoretic capacity of MIMO over the classical SISO (single input single output) systems is immediately apparent, and is explored in Chapter 2 of this thesis.

MIMO has seen considerable success urging adoption into wireless standards and into consumer products in less than a decade. The Release 7 of 3rd Generation Partnership Project (3GPP) specifications which introduced Evolved High Speed Packet Access (HSPA+) use MIMO with high-order modulation to peak at 168/22 Mbps down-link/up-link speeds. The Universal Mobile Telecommunications Systems' Long Term Evolution (UMTS-LTE) Release 8 was introduced soon after, also with a provi-

sion for up to four antennas to approach peak down-link/up-link rate of 300/75 Mbps [6]. Almost all broadband technologies of the present day either can accommodate or require MIMO systems. Local and metropolitan wireless services such as Wireless-LAN (802.11n) and WiMAX (802.16e) have, and will continue to use the technology, as a trend seen with later standards such as 802.11ac. The use of MIMO in short range (home or personal networks) ultrawideband OFDM (Orthogonal Frequency Division Multiplexing)systems has been investigated and the diversity advantages were found to be significant [7]. The following is a tabulation of some of the deployed Wireless technologies and standards that included MIMO systems [8]. The values and methodologies listed are just indicative and highly summarized to be presentable - other values and techniques may be supported. It is predicted that MIMO, coupled with affordable digital signal processing hardware, will carry wireless transmission from broadband to gigabit speeds [1].

Standards/Technologies	**Peak Rate/BW/Band**	**MIMO Methodology**
IEEE 802.11n Wi-Fi	600Mbps/40MHz/5GHz,2.4GHz	STBC, CSD, MRC[a]
IEEE 802.16 WiMAX	75Mbps/(1.25-20MHz)/(2-66GHz)	SM, STC, WF, BF
IEEE 802.20 MBWA	16Mbps/(2.5-20MHz)/(<3.5GHz)	STTD, Linear Precoding
3GPP LTE	100Mbps/(1.25-20MHz)/2.6GHz	STBC, CDD

Table 1.1: MIMO and Current Standards[1]

Some of these MIMO Methodologies will be presented in the coming sections and the rest will be defined briefly.

Unlike a traditional MIMO system, in this thesis, special constraints on either the number of modes or antennas is used. In some of the sections, a basic computational ability on the transmit side is assumed to perform a water filling operation.

1.2 Research Motivation

Previously discussed capacity scaling advantages of MIMO inspires us to explore more possibilities in the area. Performance bounds in the Shannon Theoretic sense are useful in providing a 'sanity check' for complex wireless systems, and hence it is generally worthwhile to have these at hand to monitor our expectations from Physical (PHY) and Multiple Access (MAC) layer optimizations[2].

The use of multiple antennas at the transmitter and the receiver grants us more degrees of freedom, which means that besides the option of enhancing the signal power, it is possible to mitigate interference, making MIMO suitable for mobile ad hoc Networks [2]. The scenario in which a number of MIMO nodes lie on a plane while using the same channel is of particular interest. A link in such a network is said to be experiencing co-channel interference. The problem of optimizing capacity of the whole system cannot be expected to have the same solution as that of optimizing the capacity of a single link, as the methods adopted in improving the latter are intrinsically greedy. Each link that transmits strongly to aide its own receive gain is interfering with the other links, and this intuition motivates us to delve further into the behavior of network capacity with simulations and possible theoretical ideas. In situations where the density of interfering users is a parameter than can be monitored and controlled, an optimality condition for the number can be an important decision to make. In situations where this is not possible, the transmission strategy that best suits the population of nodes can be used.

The list of WLAN standards that have integrated MIMO technologies from section 1.1 also present an insight into the need for understanding the behavior of dense wireless networks. Finally, the problem of inter-cell co-channel interference also exists in MIMO-broadcast, and although the work attempted here does not readily apply

to such a situation, some likeness of the results is evident and they might serve as a building block for future work in the area.

1.3 Previous Work

Emre Telatar (1999) laid out the foundation for the information theoretic evaluation of the MIMO system in his seminal work, [9], and a summary of the mathematical essence of MIMO capacity in this work is found in [10]. Various mathematical tools, lemmas, theorems and derivations can be found in the reference to also help the reader better absorb the material in this document. A consideration of error exponents and multiple-access in MIMO is also considered therein, which are not a part of this work. Following this, the same author has explored the impact of high node density in networks [11] and the effect of correlated channels [12]. The impact of operation in these regimes is inconclusive, but it is proposed that the impact of correlation

Extensive work on the topic of MIMO ad-hoc network capacity has been carried out by Bliss et al. A quick primer of all the related work is found in [3]. A survey of the environmental factors that influence a MIMO channel and its capacity is presented in [13], where co-operative and non-cooperative interference is considered. Also, a method of including a physical scattering model that takes into account the distance between antennas and a scatterer is presented. Because the system model that assumes a random channel matrix has an eigenvalue spectrum that is inappropriately optimistic for practical situations, channel models for a particular density of scatterers is given.

Goldsmith, A et al. (2003) present a comprehensive list of results relating to MIMO Channel capacities as well as a short treatment of MIMO multi-access channel capacities, MIMO broadcast channels, and MIMO multicell channels [14]. Although

the dealings of my work are in the PHY layer, the attempt at an extension to the MAC layer would find this reference an important tool.

Liu, J et al. (2008) pursue the exact capacity evaluation for a finite MIMO Network from a Global Optimization perspective using a branch-and-bound with reformation and linearization technique BB/RLT technique [15]. A discussion of this manner is beyond the scope of this dissertation. On the other end of the spectrum, the Chen et al. [16] and Motamedi et al. [17] show that in the case of asymptotically high densities, the network spectral efficiency is equal to n_r nats/s/Hz and is at least $n_t+n_r+2\sqrt{n_t n_r}$ nats/s/Hz in the case of Uninformed Transmitter (UT) and Informed Transmitter (IT) cases respectively. In a UT MIMO system, the transmit side receives no feedback from the receive side regarding the channel, whereas in the IT MIMO case, there is some channel information supplied. We will find it useful to take a look at these results for our analysis.

The MIMO channel spectral efficiency in the presence of interference and the facility for power control at the receiver is presented in [18]. Constant interference level at the receiver translates to a small number of high-data-rate interferers or a high number of low-data-rate interferers and finds that capacity was higher with fewer high-data-rate interferers. Chen et al. [17] also provide an asymptotic theoretical formula for the sum capacity of the network in high density of participants, but for the case of constant interference power from each of them at any receiver. Both these cases of either constant total interference power or of constant power from each interferer are useful for theoretical considerations. However, this assumption discounts the variation expected due to the physical model of the system. This dissertation includes these expected variations and verifies the consistency of the results at asymptotic limits.

At the end of Chapter 2, it will be evident that the channel capacity is a function of the singular value decomposition of the channel matrix. An asymptotic approximation

of the eigenvalue spectrum for an infinite dimension matrix is given in [19], and will be found useful in understanding some results in this work. It is worthwhile to consider this case, as the eigenvalue distribution in the case of infinite dimension matrices converge with practical systems with finite number of antennas. Another asymptotic regime is in the case of networks, where the number of nodes acting as interference increases to infinity, as does the number of receiver antennas, keeping their ratio constant. Also, the area of the universe grows accordingly to infinity, to make sure the density of the interference is kept constant. This model is discussed in [20], and is important as a tool to apply to finite systems as well.

Leveque, et al. (2005) present the Information theoretic upper bound on the capacity for such large networks [21], for a constant node density. This is one of the scenarios considered in my work, along with some results relating to varying node densities.

The effect of spatially correlated channels is an important factor to consider in the case of practical systems. In this work, the assumption that the channel coefficients across the antennas are independent is made, but the reader may refer to the work of Telatar et al. [12] for the case of correlation across the channels. Kang et al. (2003) have explored correlated fading channels and have devised the expressions for the mean and variance of the capacity and the Gaussian approximation of the capacity complementary distribution function [22]. Chiani, M et al. (2003) also evaluate the capacities for the regime of spatially correlated channel coefficients to find that the effect of exponential correlation is negligible for typical correlation coefficients, and also present a closed form for the capacity for quick evaluation of outage for such systems [23].

The treatment in this document and study of MIMO channels is under the assumption of rich scattering and hence a Rayleigh fading situation. Kang et al. (2006)

extend the results of capacity from Chapter 2 for Ricean fading in situations where there exist LOS components [24]. Rich scattering environments are favorable for MIMO Communication Systems and in this work, it is found that strong LOS components are indeed detrimental to the capacity.

1.4 Contributions

The main contributions of this work are surmised thusly.

1. A Monte-Carlo evaluation of the ergodic capacity of a MIMO ad hoc network with interference transmission by all the participants is presented.

2. A novel metric across which to evaluate the network spectral efficiency is presented, the advantage of which is better intuition of the interference profile, the possibility of comparison across different network configurations, and the attribution of more importance to some interferers over others.

3. An iterative water-filling methodology to simulate the Network Spectral Efficiency for the informed transmitter MIMO case is presented.

1.5 Organization

This thesis document is divided into 6 chapters. In Chapter 2, the MIMO channel is introduced, and the information theoretic basis for the evaluation of the capacity is presented. In chapter 3, the same is extended for MIMO systems and network capacity. In Chapter 4, the simulation results are presented. Finally, in Chapter 5, the conclusion and prospective future direction for research are given.

Chapter 2

THE MIMO CHANNEL

2.1 System Model

Consider a MIMO link in which the transmitter and the receiver have n_t and n_r antennas, respectively. The numbers $M = min(n_t, n_r)$, $N = max(n_r, n_t)$ and $t = n_r \times n_t$ need also to be kept in mind for later. Although a MIMO system is capable of operating in line-of-sight communications, its advantages are truly seen in rich multi-path scattering environments [2, 24].

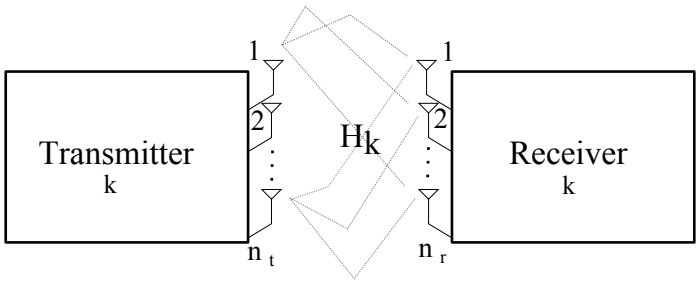

Figure 2.1: MIMO Representative System

In a flat fading channel assumption for narrowband signals, the channel between each transmit and receive antenna pair can be represented by a single complex attenuation. If $h_{m,n}$ represents the complex attenuation between antenna n at the transmitter and antenna m of the receiver, we will have $n_r \times n_t$ such gains. If k is an index we use to refer to this particular link, we have a $\mathbb{C}^{n_r \times n_t}$ matrix $\mathbf{H}_k$ whose elements are h_{mn}. The received signal $\mathbf{y}(t) \in \mathbb{C}^{n_r \times 1}$ in the presence of additive noise $\mathbf{n}(t) \in \mathbb{C}^{n_r \times 1}$ when a signal $\mathbf{s}(t) \in \mathbb{C}^{n_t \times 1}$is transmitted, is given by

$$\mathbf{y}(t) = \mathbf{H}_k \mathbf{x}(t) + \mathbf{n}(t).$$

To simplify the representation, we can consider a block of data samples and write the discrete model of the above system equation as

$$\mathbf{Y}=\mathbf{H}_k\mathbf{X} + \mathbf{N},$$

where, if there are n_s data samples, the received signal block will be $\mathbf{Y} \in \mathbb{C}^{n_r \times n_s}$, the transmit signal block $\mathbf{X}\in \mathbb{C}^{n_r \times n_s}$ and the noise $\mathbf{N} \in \mathbb{C}^{n_r \times n_s}$.

In a highly scattered environment with no LOS component, each $h_{m,n}$ can be modeled as a zero-mean complex Gaussian with variance 0.5, and each h is independent of the other, as discussed in Chapter 1. This also implies that the magnitude of the elements are Rayleigh distributed and will have uniform phase.

2.2 SISO Capacity

For a single-Input, single-Output system, the discrete model is given by

$$\underline{\mathbf{y}} = h\underline{\mathbf{x}} + \underline{\mathbf{n}},$$

and the capacity for this system when the signal-to-noise ratio is γ is given by [26]

$$c_{SISO} = \log_2(1 + \gamma|h|^2).$$

When the channel is random, the ergodic capacity is found by taking an expectation with respect to the distribution of the channel gain. In the case of the real variable SISO channel capacity, the expression was of the form $\frac{1}{2}\log_2(1 + \gamma)$ per complex dimension. This thesis deals with complex baseband signals, and hence the half disappears.

2.3 Uninformed Transmitter MIMO Capacity

As defined earlier, an uninformed transmitter MIMO system is the one in which the transmit side receives no clue about the channel from the receiver. We take a small

detour to derive an important and recurring result regarding the complex gaussian probability density function $S_X(\mathbf{x})$ with a covariance $\mathbf{Q}$:

$$S_X(\mathbf{x}) = |\pi\mathbf{Q}|^{-1} e^{-\mathbf{x}^\dagger \mathbf{Q}^{-1}\mathbf{x}}$$

We have the differential entropy of $\mathbf{x}$ as[9],

$$\begin{aligned}
\mathcal{H}(S) &= \mathcal{E}_S[-\log_2(S(\mathbf{x}))] \\
&= \log_2(|\pi\mathbf{Q}|) + (\log_2 e)\mathcal{E}_S[\mathbf{x}^\dagger Q^{-1}\mathbf{x}] \\
&= \log_2(|\pi\mathbf{Q}|) + (\log_2 e) tr(\mathcal{E}_S[\mathbf{x}\mathbf{x}^\dagger]\mathbf{Q}^{-1}) \\
&= \log_2 |\pi e\mathbf{Q}|. \qquad (2.1)
\end{aligned}$$

Where $\mathcal{E}_s$ is the expectation with respect to the pdf $S_X(\mathbf{x})$. Here, we have used the equivalences $\mathcal{E}[\mathbf{x}^\dagger\mathbf{x}] = tr(\mathcal{E}[\mathbf{x}\mathbf{x}^\dagger])$ and $\mathcal{E}_S[\mathbf{x}\mathbf{x}^\dagger] = Q$. The † symbol is used to represent Hermitian Conjugate. Another important result (the proof of which can be found in [9]) is that when $S_X(\mathbf{x})$ is a Zero-Mean Circularly Symmetric Complex Gaussian, the entropy is maximized. i.e., $\mathcal{H}(p) \leq \mathcal{H}(S)$ for any $p_X(\mathbf{x})$. We must not forget that the differential entropy is a function of the distribution only. With these results at hand, the capacity of a MIMO link can be determined.

By definition, the capacity of the MIMO channel is the maximum mutual information between the input and the output to the channel[9] ,

$$\mathcal{I}(\mathbf{X};\mathbf{Y}) = \mathcal{H}(\mathbf{Y}) - \mathcal{H}(\mathbf{Y}|\mathbf{X}).$$

The second term is simply the entropy of the noise and the first term is evaluated by finding the Covariance of Y as:

$$\begin{aligned}
\mathcal{E}[\mathbf{Y}\mathbf{Y}^\dagger] &= \mathcal{E}[(\mathbf{H}_k\mathbf{X} + \mathbf{N})(\mathbf{H}_k\mathbf{X} + \mathbf{N})^\dagger] \\
&= \sigma_n^2\mathbf{I}_{n_r} + \mathbf{H}_k\mathbf{Q}\mathbf{H}_k^\dagger \qquad (2.2)
\end{aligned}$$

Note that if X is Circularly Symmetric Complex Gaussian, so is $\mathbf{Y}$, and this is the entropy maximizing condition. Also, if we consider the noise to be complex additive white Gaussian noise with covariance $\sigma_n^2\mathbf{I}_{n_r}$, then we may use the result (2.1) to evaluate the mutual information as

$$\begin{aligned}\mathcal{I}(X;Y) &= \log_2\left|\pi e(\sigma_n^2\mathbf{I}_{n_r} + \mathbf{H}_k\mathbf{Q}\mathbf{H}_k^\dagger)\right| - \log_2\left|\pi e\sigma_n^2\mathbf{I}_{n_r}\right| \\ &= \log_2\left|\frac{\pi e(\sigma_n^2\mathbf{I}_{n_r} + \mathbf{H}_k\mathbf{Q}\mathbf{H}_k^\dagger)}{\pi e\sigma_n^2\mathbf{I}_{n_r}}\right| \\ &= \log_2\left|\mathbf{I}_{n_r} + \frac{\mathbf{H}_k\mathbf{Q}\mathbf{H}_k^\dagger}{\sigma_n^2}\right| \end{aligned} \tag{2.3}$$

Therefore, the capacity is:

$$C = \max_{Q} \log_2\left|\mathbf{I}_{n_r} + \frac{\mathbf{H}_k\mathbf{Q}\mathbf{H}_k^\dagger}{\sigma_n^2}\right|$$

Now, from the properties of Covariance Matrices, $\mathbf{Q}$ is positive semidefinite and can be written as $\mathbf{Q} = \mathbf{U}\mathbf{Q}_D\mathbf{U}^\dagger$, where $\mathbf{Q}_D$ is a diagonal matrix and $\mathbf{U}$ is unitary. This preserves the mutual information expression from (2.3) as is, because unitary transformation on $\mathbf{H}_k$ does not change its distribution. Hence we may rewrite the equation as before, using a diagonal transmit covariance matrix without loss.

$$\begin{aligned} C &= \max_{\mathbf{Q}_D} \log_2\left|\mathbf{I}_{n_r} + \frac{\tilde{\mathbf{H}}_k\mathbf{Q}_D\tilde{\mathbf{H}}_k^\dagger}{\sigma_n^2}\right| \\ &= \max_{\mathbf{Q}\,:\,\mathrm{tr}(\mathbf{Q})\leqslant \mathrm{P}} \log_2\left|\mathbf{I}_{n_r} + \frac{\mathbf{H}_k\mathbf{Q}\mathbf{H}_k^\dagger}{\sigma_n^2}\right|, \end{aligned} \tag{2.4}$$

Where we have also added a power constraint to the maximization by making sure that the total transmit power is less than or equal to a chosen P. Without this, there is no meaning for the maximization as we can increase the power to get a higher capacity

at all times. Equation (2.4) is the final expression of the *instantaneous* capacity of the MIMO channel. Now the maximum is reached when $\mathbf{Q}$ is equal to $\frac{P}{n_t}\mathbf{I}_{n_t}$ [9].

That is, when the transmit power is distributed equally amongst all the antennas, the best possible capacity is achieved. However, this is only the case for a transmitter that does not have any information about the channel as feedback from the receiver. We will hence call this the Uninformed Transmitter capacity.

$$C_{UT} = \log_2 \left| \mathbf{I}_{n_r} + \frac{\mathrm{P}}{n_t} \frac{\mathbf{H}_k \mathbf{H}_k^\dagger}{\sigma_n^2} \right| \tag{2.5}$$

Finally, we can write the *Ergodic* capacity of the uninformed transmitter MIMO channel as below

$$C_{UT} = \mathcal{E}_H \left\{ \log_2 \left| \mathbf{I}_{n_r} + \frac{\mathrm{P}}{n_t} \frac{\mathbf{H}_k \mathbf{H}_k^\dagger}{\sigma_n^2} \right| \right\}. \tag{2.6}$$

Figure 2.2 illustrates the variation of channel capacity as a function of the SNR (P/σ_n^2) for various MIMO configurations. As one would expect, higher SNRs perform better, as does increasing the number of antennas. We clearly see the improvement being drastic over SISO, SIMO (receive diversity), and MISO (transmit gain) in the case of the 2×2 MIMO system. Also, the capacity multiplicative effect is observed upon increasing the number of antennas. To get a sense of this phenomenon, we can evaluate the capacity in the limit of large number of transmit antennas. In this case, $\frac{1}{n_t}\mathbf{H}_k\mathbf{H}_k^\dagger \longrightarrow \mathbf{I}_{n_r}$, and the capacity becomes

$$\begin{aligned} C_{UT} &= \mathcal{E}_H \left\{ \log_2 \left| \mathbf{I}_{n_r} + \frac{\mathrm{P}}{n_t} \frac{\mathbf{I}_{n_r}}{\sigma_n^2} \right| \right\} \\ &= n_r \log_2 \left(1 + \frac{\mathrm{P}}{n_t \sigma_n^2} \right), \end{aligned} \tag{2.7}$$

which is just the SISO system capacity multiplied by the number of receive antennas.

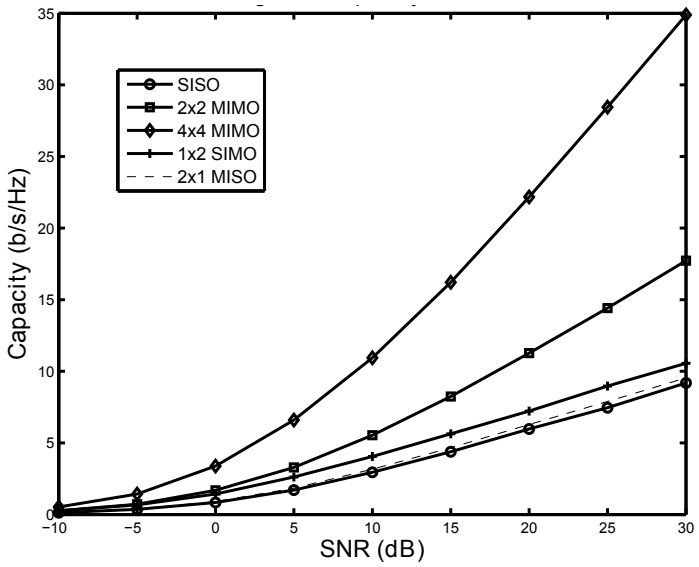

Figure 2.2: UT Ergodic Capacity of Isolated MIMO Links

At this point, it is pertinent to note that the use of 'channel capacity' is not as a universal spectral efficiency bound, but is defined in the context of the system under consideration. That is, although it might be possible to achieve a higher spectral efficiency bound for the *channel*, under the given constraints on what the transmitter knows and the power it uses to transmit, the definition of capacity might be different for the system. Intuitively, we should be able to achieve a higher capacity in the presence of channel knowledge. This is indeed the case, and this condition will be pursued next.

2.4 Informed Transmitter MIMO Capacity

In the case of the IT MIMO system, the transmitter is supplied information, known as the channel state through feedback by the receiver, and using (2.4), the transmit covariance is changed to maximize the capacity. The nature of this information makes a lot of difference in the achievable channel capacity- the distribution of the channel, the nature of the channel, or the channel itself can be fed back. In this study, the

assumption is that the transmitter is given the 'link-CSI', which is the instantaneous channel between the transmitter and the receiver. Various methods exist to estimate the channel at the receiving end, some of which are discussed in [2, 25].

The following is a brief outline of the mathematical background that will be immediately useful. The function $\lambda_{\mathbf{J},m}$ extracts the m^{th} largest eigenvalue of the matrix $\mathbf{J}$, and we will hence represent the SNR by ρ.

1. Singular Value Decomposition of the Channel Matrix: The channel matrix can be decomposed as

$$\mathbf{H}_k = \mathbf{U}\mathbf{D}\mathbf{V}^\dagger,$$

where $\mathbf{U}$ and $\mathbf{V}$ are unitary matrices and $\mathbf{D}$ is a diagonal matrix of singular values of $\mathbf{H}_k$. This means that the System Model can be rewritten, but now with a channel matrix with only diagonal elements, as shown below:

$$\mathbf{Y} = \mathbf{H}_k\mathbf{X} + \mathbf{N}$$

$$\mathbf{Y} = \mathbf{U}\mathbf{D}\mathbf{V}^\dagger\mathbf{X} + \mathbf{N}$$

$$\mathbf{U}^\dagger\mathbf{Y} = \mathbf{D}\mathbf{V}^\dagger\mathbf{X} + \mathbf{U}^\dagger\mathbf{N}$$

$$\tilde{\mathbf{Y}} = \mathbf{D}\tilde{\mathbf{X}} + \tilde{\mathbf{N}}$$

This means that using SVD, we have arrived at an alternate representation of the MIMO system that is equivalent to a set of $M = min(n_t, n_r)$ SISO systems (because $\mathbf{D}$ has M non-zero diagonal elements). The capacity of the MIMO

System is just the sum of the capacities of the M equivalent SISO systems:

$$\begin{aligned} C_{UT,m} &= \log_2 \left| \mathbf{I}_{n_r} + \frac{\mathrm{P}}{n_t} \frac{\mathbf{H}_k \mathbf{H}_k^\dagger}{\sigma_n^2} \right| \\ &= \sum_{m=1}^{M} \mathcal{E}_H \left\{ \log_2 \left(1 + \frac{\mathrm{P}}{n_t} \frac{\lambda_{\mathbf{H}_k \mathbf{H}_k^\dagger, m}}{\sigma_n^2} \right) \right\} \\ &= \sum_{m=1}^{M} \mathcal{E}_H \left\{ \log_2 \left(1 + \frac{\rho^2 d_m^2}{n_t} \right) \right\}, \end{aligned} \tag{2.8}$$

where d_m is the m^{th} diagonal element of $\mathbf{D}$. This is possible because unitary transformations on the zero mean circularly symmetric complex gaussian (ZMCSCG) noise $\mathbf{N}$ and $\mathbf{X}$ preserve their distributions.

2. Unitary transformation of ZMCSCG preserves its distribution: A linear transformation of a Gaussian matrix is still a Gaussian matrix. However, we can see with the example of the noise matrix, that the variance also remains the same for the matrix $\mathbf{N}' = \mathbf{U}\mathbf{N}$ when $\mathbf{U}$ is unitary:

$$\begin{aligned} \mathcal{E}[\mathbf{N}'\mathbf{N}'^\dagger] &= \mathcal{E}[\mathbf{U}\mathbf{N}\mathbf{N}^\dagger\mathbf{U}^\dagger] \\ &= \mathbf{U}\mathcal{E}[\mathbf{N}\mathbf{N}^\dagger]\mathbf{U}^\dagger \\ &= \sigma_{\mathbf{N}}^2 \mathbf{U}\mathbf{U}^\dagger \\ &= \sigma_{\mathbf{N}}^2 \mathbf{I} \end{aligned} \tag{2.9}$$

3. Matrix Approximations: In the context of the capacity expressions that we encounter in this document, a few matrix approximations come in handy. Firstly, we see the value of $\log_2 |1 + \mathbf{X}|$ when $\mathbf{X}$ is small. Because $|\mathbf{X}| = \prod_m \lambda_{\mathbf{X},m}$ and

because $\lambda_{(\mathbf{I}+\mathbf{X}),m} = 1 + \lambda_{\mathbf{X},m}$, we have:

$$\begin{aligned} c &= \log_2 |1 + \mathbf{X}| \\ &= \log_2 \left[\prod_m (1 + \lambda_{\mathbf{X},m}) \right] \\ &= \sum_m \log_2(1 + \lambda_{\mathbf{X},m}) \\ &\approx \log_2(e) \sum_m \lambda_{\mathbf{X},m}, \end{aligned} \tag{2.10}$$

for which we used the approximation $\ln(1 + x) \approx \ln(x)$ for small x.

Secondly, consider the Hermitian Matrix $\mathbf{X}$ (i.e., $\mathbf{X}^\dagger = \mathbf{X}$)with the eigenvalue decomposition $\mathbf{X} = \mathbf{U}\Lambda\mathbf{U}^\dagger$, it suffices to know the approximation for this matrix when raised to a large power:

$$\mathbf{X}^k = \sum_{m=1}^{M} \lambda_{\mathbf{X},m}^k \mathbf{u}_m \mathbf{u}_m^\dagger, \tag{2.11}$$

where $\mathbf{u}_i$ is the eigenvector corresponding to the m^{th} eigenvalue and is also the column m of $\mathbf{U}$.

Now it is easy to extend the capacity to the case of an informed transmitter. From the previous introduction to the Singular Value Decomposition of the channel matrix, we have the decomposed form:

$$\mathbf{H}_k = \mathbf{U}\mathbf{D}\mathbf{V}^\dagger,$$

where $\mathbf{V}$ is a $n_t \times n_t$ unitary matrix. In the equivalent linear model, we transmit $\tilde{\mathbf{X}}$ whose covariance is given by

$$\mathbf{Q} = \mathbf{V}\mathbf{P}\mathbf{V}^\dagger,$$

where P is a diagonal matrix with the M elements, $\lambda_{\mathbf{Q},i}$. Hence, the capacity is now

written as:

$$C_{IT} = \sum_{m=1}^{M} \log_2 \left(1 + \frac{\lambda_{B,m}\lambda_{W,m}}{\sigma^2}\right)$$
$$= \sum_{m=1}^{M} \log_2 \left(1 + \frac{p_m d_m^2}{\sigma^2}\right) \tag{2.12}$$

The trick now is to optimize the transmit covariance matrix (and hence $\lambda_{\mathbf{X},m}$) so as to achieve the maximum capacity, under the constraint that the sum of allocated powers across all the streams is at most equal to the total power, P. This is done by the method of constrained optimization with Lagrange multipliers [27] as briefly discussed below.

Consider the Lagrangian for the channel capacity,

$$\Phi(p_1, p_1, ...p_M, \mu) = \sum_{m=1}^{M} \log_2 \left(1 + \frac{p_m d_m^2}{\sigma^2}\right) + \mu(\mathrm{P} - \Sigma p_m)$$

Maximizing this function w.r.t one of the subchannel powers, p_k gives:

$$\frac{\mathrm{d}\Phi}{\mathrm{d}p_k} = \frac{d_k^2/\sigma^2}{1 + p_k d_k^2/\sigma^2} - \mu = 0$$

Therefore, we get the optimum choice of the power allocation to be

$$p_k = \left(\frac{1}{\mu} - \frac{\sigma^2}{d_k^2}\right)^+$$

Where we use the function $(z)^+$ to mean $max(0, z)$ because power values cannot be negative in this context. As the arrangement of the eigenvalues of the channel matrix was in the descending order, the successive values of the terms σ^2/d_i^2 will be in the ascending order. Of the m non-zero modes, only some of them 'qualify' for power allocation, in the sense that the value of the respective p_k will be greater than zero. If the total available power is imagined to be a certain volume of water while the σ^2/d_i^2 terms are walls with heights representative of their values, there is a 'water-filling' analogy to be found in the optimization condition and this is represented in figure 2.3.

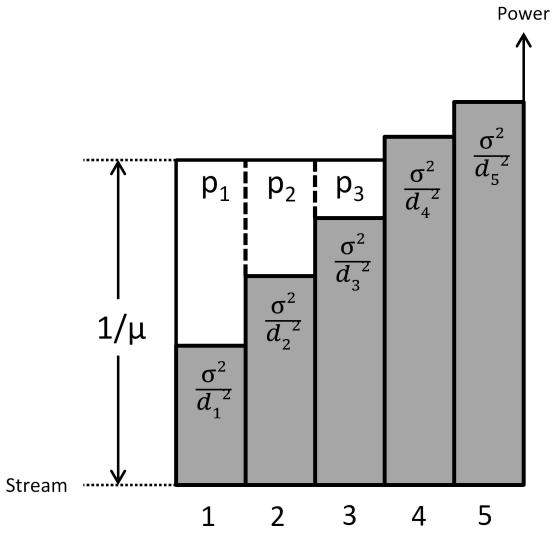

Figure 2.3: Water-filling Power Allocation

It is now imperative to see the capacity improvement gained in adding a water-filling step to the transmission procedure. We hence evaluate the capacity ratio C_{IT}/C_{UT}, as this represents the gain that was achieved. To make sense of the simulation results presented in figure 2.4, consider the region of high SNR - where the distribution of the power with water-filling would be almost same (with the bars in figure 2.3 being very tall, and hence not making a difference in their values) and hence would be very similar to the equal power transmission capacity. Therefore, the ratio will be near to 1. On the other hand, at low SNR, all the power in water-filling will be allocated to one mode (one small bar of power at the first stream) and by using the approximation $\log(1+x) = x$ for small x, we get the capacity ratio to be:

$$\begin{aligned} C_{RATIO} &= \frac{\log_2(1+\rho d_1^2)}{tr\{\log_2(1+\frac{\rho}{n_t}HH^\dagger)\}} \\ &\approx n_t \frac{d_1^2}{tr\{HH^\dagger\}} \end{aligned}$$

Hence, the capacity improvement can be at most equal to n_T with water-filling. This happens when there is a dominant eigenvalue and $tr\{HH^{\dagger}\} \approx d_1^2$ and when the channel is rank one (MISO case).

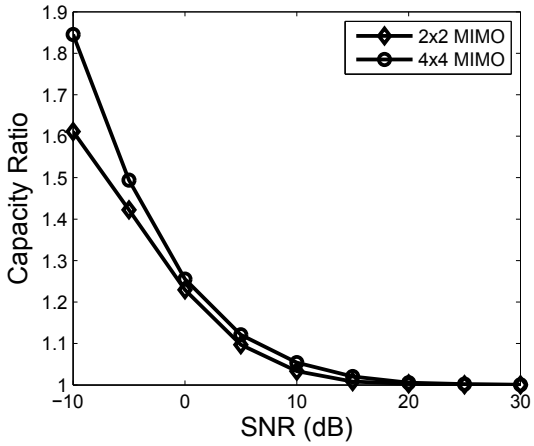

Figure 2.4: Simulated Capacity Ratio C_{IT}/C_{UT}

2.5 Capacity Enhancement Through Spatial Diversity

With the facility of multiple antennas at either ends of the communication system, the major advantage that is obtained is spatial diversity. The figure below shows the three most obvious spatial diversity techniques used. This summary can accompany Table 1.1 in explaining the advantages of MIMO methodologies. With receiver diversity, no special coding is required and the gain obtained is reduction of error due to the presence of multiple copies of the data. Many methods exist to make the best of these copies - either choose the highest SNR (switch diversity/selection combining) or linearly combine them to make a decision (maximum ratio combining). With transmit diversity, space-time coding is required to optimally transmit data repeatedly over the transmit antennas. The transmit gain is inherent in this redundancy. Finally, the full spatial multiplexing MIMO case uses multiple streams, whose copies

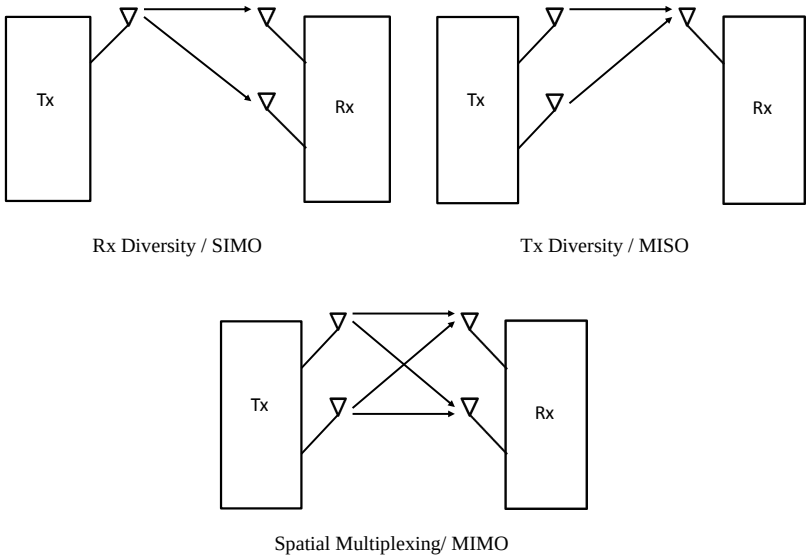

Figure 2.5: Spatial Diversity Techniques

are received at multiple antennas, making it the most robust technique whilst having more hardware and coding requirements.

2.6 Outage Capacity

With the assumption of a stochastic channel model, the Capacity, which is a function of the channel, is also a stochastic variable [2]. If it is known that error-free transmission is not possible below a particular rate, we can get the channel ν-outage capacity to be C_ν, where

$$\Pr\{\mathrm{C}(\mathbf{H}) \leq \mathrm{C}_\nu\} = \nu$$

Another approach to arrive at a metric that represents the same performance parameter is when we define the probability of a successful or 'closed' link. If the instantaneous channel capacity is higher than a particular rate R, the channel performance is as desired, and is said to be closed. In such an event, the probability of

close is given by

$$\Pr\{\mathrm{C}(\mathbf{H}) \geq R\} = \mathrm{P}_{close}$$

Both the definitions of Outage Capacity are used in literature and it is assumed that the correct one is picked up from the context. Expectedly, the former definition is used for a small outage probability and the latter for high probability of close. Also, one may protest about the name *outage capacity* , because clearly, the capacity occurs when there is no outage but it is merely a matter of convention.

Armed with the mathematical approach to derive the channel capacity of a single link, it is simple to extend the same to the case of a MIMO Network capacity.

Chapter 3

MIMO CHANNEL IN INTERFERENCE

The capacity enhancement achieved with multiple antennas was established in Chapter 2 for single links. Such isolated communication systems rarely exist, and it is always expected that some interference shall impair a transmit-receive link. When the interference uses the same frequency band - as is the case with almost all general frequencies in deployment, co-channel interference results. All the nodes in the network (or *system* to indicate that PHY layer is under consideration) experience interference but a common approach is to consider a single link and see the adverse effects of interference on it, and then extend it to the system under the assumption that the same adversity is seen by all the nodes. This representative node pair is referred to as the *link of interest* in this text, and the corresponding Receiver is the *node of interest*. The distance between the transmit-receive pair of the link of interest on a plane is called the *link radius*. If it is true that the effect of an interference can be ignored as long as it is at a particular distance from the node of interest in the presence of path loss, the effective universe that needs to be considered is a circular plane of this radius. It will later be shown that it is indeed true that certain interferences can be ignored.

If we consider a unit variate noise, then the noise normalized receive powers will represent the SNR and this approach is easier to represent. Hence, if there are L identical nodes in the representative universe, the discrete time signal model for the L^{th} link is given by

$$\mathbf{y}_L = \sqrt{\rho_L}\mathbf{H}_{L,L}\mathbf{x}_L + \sum_{j=1}^{L-1} \sqrt{\rho_j}\mathbf{H}_{L,j}\mathbf{x}_j + \mathbf{n}, \tag{3.1}$$

where $\mathbf{H}_{m,n}$ is the channel between the n^{th} receiver and the m^{th} transmitter. The system capacity is the sum of all the participating link capacities. It becomes apparent why this might be a tough problem to crack - the interference powers seen by each of the nodes might very different and at the same time, the number of participating nodes in the representative universe for each of these might also change and there is not one case that is more correct than another. We hence need to make some assumptions regarding the problem. First of all, if we assign a particular probability density function for the location of the nodes in the plane, we can limit the variability and also control it for simulations. Secondly, having a predefined distribution for the node locations means that we can also assume that the interference effects seen on one link are similar to those of the other, but in their own (similar) representative universes. Hence, the system capacity is simplistically the capacity of a single link multiplied by the number of participating links, a concept that will be further reinforced in the upcoming chapter.

3.1 MIMO Link Capacity in Interference

The capacity of a MIMO link in the presence of interference is derived from (4.1) and the mutual information $\mathcal{I}(x;y) = \mathcal{H}(y) - \mathcal{H}(y|x)$. The sum of all the interference (colored noise) and the additive noise can be written as a combined noise term $\mathbf{z}$.

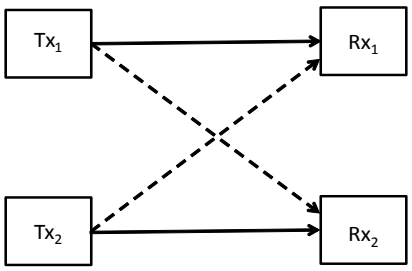

Figure 3.1: The Simplest System (Having One Interfering Node)

This term is rewritten below for convenience.

$$\mathbf{z} = \sum_{j=1}^{L-1} \sqrt{\rho_j}\mathbf{H}_{L,j}\mathbf{x}_j + \mathbf{n}$$

The covariance matrix of the Interference plus Noise is then obtained to be

$$\begin{aligned}
\mathbf{R_{zz}} &= \mathcal{E}[\mathbf{z}\mathbf{z}^\dagger] \\
&= \mathcal{E}[(\sum_{j=1}^{L-1} \sqrt{\rho_j}\mathbf{H}_{L,j}\mathbf{x}_j + \mathbf{n})(\sum_{j=1}^{L-1} \sqrt{\rho_j}\mathbf{H}_{L,j}\mathbf{x}_j + \mathbf{n})^\dagger] \\
&= \mathbf{I}_{n_r} + \sum_{j=1}^{L-1} \rho_j \mathbf{H}_{L,j}\mathbf{Q}_j\mathbf{H}_{L,j}^\dagger
\end{aligned} \tag{3.2}$$

The covariance matrix $\mathbf{R_{yy}}$ for the received signal $\mathbf{y}_L$ now becomes

$$\begin{aligned}
\mathbf{R_{yy}} &= \mathcal{E}[\mathbf{y}\mathbf{y}^\dagger] \\
&= \mathcal{E}[(\sqrt{\rho_{_L}}\mathbf{H}_L\mathbf{x} + \mathbf{w})(\sqrt{\rho_{_L}}\mathbf{H}_L\mathbf{x} + \mathbf{w})^\dagger] \\
&= \mathbf{R}_{zz} + \rho_{_L}\mathbf{H}_L\mathbf{Q}_L\mathbf{H}_L^\dagger
\end{aligned} \tag{3.3}$$

We have discarded the notation $\mathbf{H}_{L,L}$ in favor of just $\mathbf{H}_L$ because this will be a repeatedly used term and because it is unique to the link. In arriving at these expressions, it was assumed that the noise vector $\mathbf{n}$ and the channels were independent, that the nodes use a Gaussian codebook and that the transmissions are independent of each other [28]. Also, the entries of $\mathbf{H}_{m,n}$ and $\mathbf{H}_{m,k}$ are independent for $n \neq k$. All these assumptions are valid when each transmission is done without any knowledge of the other transmissions and with uncorrelated channels. Because the power term is written as a coefficient, it is important to note that $\mathrm{tr}\{\mathbf{Q}_k\} = 1$ for all the L transmitters. Similar to the situation in Section 2.3, it is easy to see that $\mathbf{w}$ and $\mathbf{y}_L$ are Gaussian distributed with the covariance matrices $\mathbf{R_{zz}}$ and $\mathbf{R_{yy}}$ respectively.

Therefore the Mutual Information is,

$$\begin{aligned}\mathcal{I}(\mathbf{x};\mathbf{y}) &= \log_2\left|\pi e\left(\mathbf{R}_{zz}+\rho_{_L}\mathbf{H}_L\mathbf{Q}_L\mathbf{H}_L^\dagger\right)\right| - \log_2\left|\pi e\mathbf{R}_{zz}\right| \\ &= \log_2\left|\frac{\pi e\left(\mathbf{R}_{zz}+\rho_{_L}\mathbf{H}_L\mathbf{Q}_L\mathbf{H}_L^\dagger\right)}{\pi e\mathbf{R}_{zz}}\right| \\ &= \log_2\left|\mathbf{I}_{n_r}+\rho_{_L}\mathbf{R}_{zz}^{-1}\mathbf{H}_L\mathbf{Q}_L\mathbf{H}_L^\dagger\right| \end{aligned} \tag{3.4}$$

Also, using the property $\log|I+AB| = \log|I+BA|$, we can get an alternate form,

$$\mathcal{I}(\mathbf{x};\mathbf{y}) = \log_2\left|\mathbf{I}_{n_r}+\rho_{_L}\mathbf{R}_{zz}^{-\frac{1}{2}}\mathbf{H}_L\mathbf{Q}_L\mathbf{H}_L^\dagger\mathbf{R}_{zz}^{-\frac{1}{2}}\right| \tag{3.5}$$

Hence the capacity is obtained by maximizing this expression across the transmit matrix $\mathbf{Q}_L$ under the constraint that $\mathrm{tr}\{\mathbf{Q}_L\} = 1$. It is important to be remember that the goal of this section is to focus on a greedy maximization of the link's own capacity with some assumptions about, but no control over the transmissions of the other nodes. Hence, there is only a possibility of maximizing over $\mathbf{Q}_L$. Before considering the cases for informed and uninformed transmitter capacities, an alternate but more intuitive approach to the same result as above is presented.

3.2 Whitening the Channel

In the case of no interference, the results derived were when the noise was white. If, with a 'whitening' transformation, we could get rid of the colored noise (spatially distributed interference), we can easily apply the same results again. In other words, we treat the interference as a Gaussian noise and whiten it [29]. This is possible because of the assumptions made in arriving at (3.3). This is done by multiplying the received signal vector by $\mathbf{R}_{zz}^{-1/2}$:

$$\begin{aligned}\mathbf{R}_{zz}^{-1/2}\mathbf{y}_L &= \sqrt{\rho_{_L}}\mathbf{R}_{zz}^{-1/2}\mathbf{H}_L\mathbf{x}_L + \mathbf{R}_{zz}^{-1/2}\mathbf{z} \\ \tilde{\mathbf{y}} &= \sqrt{\rho_{_L}}\tilde{\mathbf{H}}_L\mathbf{x}_L + \tilde{\mathbf{z}}\end{aligned} \tag{3.6}$$

The distribution of the channel matrix $\tilde{\mathbf{H}}_L$ is still the same, and the covariance of $\tilde{\mathbf{z}}$ is

$$\begin{aligned}\mathcal{E}[\tilde{\mathbf{z}}\tilde{\mathbf{z}}^\dagger] &= \mathcal{E}[(\mathbf{R}_{zz}^{-1/2}\mathbf{z})(\mathbf{R}_{zz}^{-1/2}\mathbf{z})^\dagger] \\ &= \mathbf{R}_{zz}^{-1}\mathcal{E}[\mathbf{z}\mathbf{z}^\dagger] \\ &= \mathbf{I}_{n_r},\end{aligned}$$

which is the result of whitening the interference. Hence, as in Chapter 2, the mutual information can be written with the channel being $\tilde{\mathbf{H}}_L$and with no interference:

$$\begin{aligned}\mathcal{I}(\mathbf{x};\mathbf{y}) &= \log_2\left|\mathbf{I}_{n_r} + \rho_{_L}\tilde{\mathbf{H}}_L\mathbf{Q}_L\tilde{\mathbf{H}}_L^\dagger\right| \\ &= \log_2\left|\mathbf{I}_{n_r} + \rho_{_L}\mathbf{R}_{zz}^{-\frac{1}{2}}\mathbf{H}_L\mathbf{Q}_L\mathbf{H}_L^\dagger\mathbf{R}_{zz}^{-\frac{1}{2}}\right|,\end{aligned}$$

which is the same as (3.5), since $\mathbf{R}_{zz}^{-1/2}$ is Hermitian. Hence, the results from Chapter 2 for no interference situation can be extended now, but with a whitened matrix.

3.3 Uninformed Transmitter MIMO Capacity with Interference

As before, the best possible blind transmission scheme is to divide the power equally amongst all the antennae. Again, the receiver is aware of the channel, is able to estimate the interference and hence the interference-plus-noise covariance. This will be all the state information required to whiten the channel. Hence, the ergodic capacity for the uninformed transmitter is given by:

$$\begin{aligned}C_{UT} &= \mathcal{E}_H\left\{\log_2\left|\mathbf{I}_{n_r} + \frac{\rho_{_L}}{n_t}\mathbf{R}_{zz}^{-\frac{1}{2}}\mathbf{H}_L\mathbf{H}_L^\dagger\mathbf{R}_{zz}^{-\frac{1}{2}}\right|\right\} \\ &= \mathcal{E}_H\left\{\log_2\left|\mathbf{I}_{n_r} + \frac{\rho_{_L}}{n_t}\mathbf{R}_{zz}^{-1}\mathbf{H}_L\mathbf{H}_L^\dagger\right|\right\}. \qquad (3.7)\end{aligned}$$

3.4 Informed Transmitter MIMO Capacity with Interference

Again, we can use the same results as in section 2.4 to the interference inclusive MIMO case, but now with a whitened channel. The water-filling algorithm now not only has to transmit such that higher powers are poured into the channel streams with lower attenuation, but also to be louder than the interfering transmit streams. This is inherent in the multiplication by $\mathbf{R}_{zz}^{-1}$.

$$\begin{aligned}\mathbf{C}_{IT} &= \sum_{i=1}^{m} \log_2 \left(1 + \frac{\lambda_{\mathbf{Q},i}\lambda_{\tilde{\mathbf{W}},i}}{\sigma^2}\right) \\ &= \sum_{i=1}^{m} \log_2 \left(1 + \rho_i \tilde{d}_i^2\right), \end{aligned} \tag{3.8}$$

where $\tilde{d}_i^2$ are the squares of the i^{th} eigenvalues of the whitened channel matrix, and the ρ_i are the SNR allocation to each stream as derived through water-filling algorithm. Figure 3.2 below shows the effect of increasing Interference power, with only one interferer on the informed and the uninformed transmit capacity.

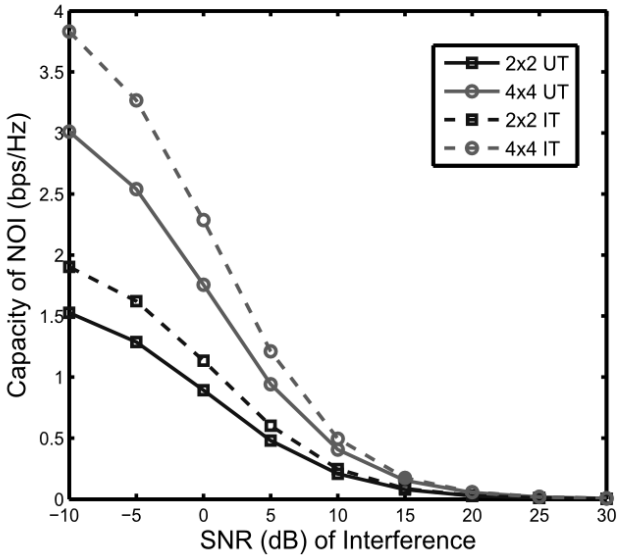

Figure 3.2: Channel Capacity in the Presence of Interference, NOI SNR = 0dB

Figure 2.2 should convince us that the interfering node in this scenario has an increasing capacity as its SNR is being increased. One can expect a similar curve when the number of interferers increases, all with the same power. This is an unrealistic case, especially in ad hoc networks, as this is a condition where there is power control by the transmitters. This can, however, happen at the base station in the case of multi user uplink in cellular systems. A more interesting scenario is the case of the power control at the receivers of ad-hoc systems, in which the total interference power is restricted to a particular level, possibly with the help of single user detection. In [18], this analysis is carried out for the case when the power from the interferers and the intended transmission is fixed at 20dB over the noise floor. Theoretical analysis is not presented in the reference, but it is attempted in Section 4.5. The result is presented here for the case of $2x2$ and $4x4$ MIMO. Most importantly, we observe that the curve can be interpreted to say that the NOI is in a better situation with a few high-data-rate interferers than it is with a large number of low-data-rate interferers.

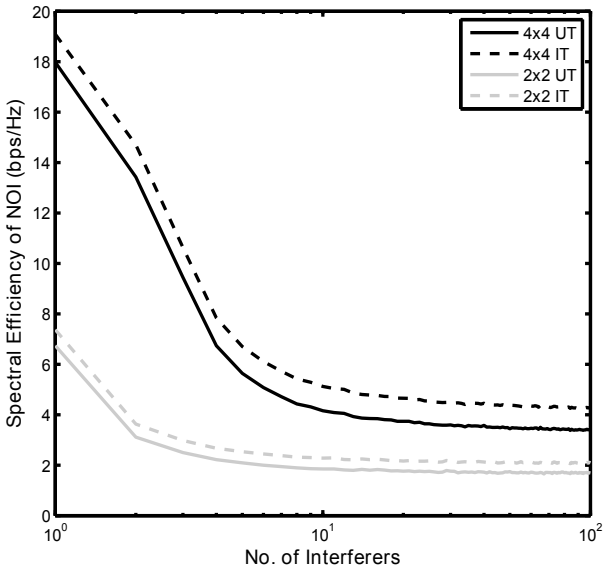

Figure 3.3: Spectral Efficiency of NOI with Total Interference Power Constraint

Chapter 4

MIMO NETWORK CAPACITY

After considering the cases of the single user MIMO channel and the response of this channel to the presence of interference, the case of the system capacity arises. As was shown in section 3.4 for the simplest case of 2 pairs of nodes, increasing the SNR is not the ultimate answer. Blindly supplying high powers in a network means that each participating link is being loud, hence interfering with the other transmissions. Also, in most practical systems, the transmitters are limited in power and the optimization has to be done under the assumption that altering the power is not an option. The optimization is done yet again over the transmit covariance, but only, instead of considering one of the covariance matrices, we have to optimize such matrices over all users so as to get an overall maximum mutual information.

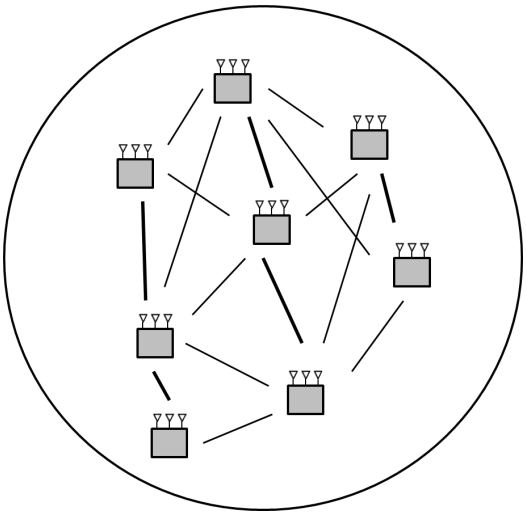

Figure 4.1: Interference in a MIMO Network

4.1 System Model

It is extremely difficult and impractical to have co-ordinated and completely co-operating nodes in an ad hoc network due to the lack of any central node to act as a mediator. It is not possible to perfectly partition the time-frequency spaces so as to not interfere with an unintended receiver. Hence, a minimal amount of cooperation is expected from each node, and the expectation is that any reduction in the interference is motivated by improving the capacity of the link itself.

This means that the capacity of the system is simply the sum of all the individual capacities operating in parallel. The system model of (3.1) is written here again for the link L, with a slight alteration to show the source and the recipient of an interference through the indices of the attenuation/SNR term. This will let us write the sum capacity easily.

Some assumptions that will be used in the derivations that immediately follow are given below. More parameters used in the simulations will be presented in Chapter 5.

1. The channels for all interference signals are independent of each other and the channel of the link of interest.

2. The noise is additive Zero-mean circularly symmetric complex gaussian with covariance $\sigma^2\mathbf{I}$.

3. Each $\rho_{j,k}$represents SNR when $j = k$ and Interference to Noise Ratio (INR) when $j \neq k$.

$$\mathbf{y}_L = \sqrt{\rho_{L,L}}\mathbf{H}_{L,L}\mathbf{x}_L + \sum_{j=1}^{L-1} \sqrt{\rho_{L,j}}\mathbf{H}_{L,j}\mathbf{x}_j + \mathbf{n}, \tag{4.1}$$

4.2 Sum Capacity of the System

It is straightforward to write the sum mutual information as

$$\begin{aligned}\mathcal{I}_{_{network}}(\mathbf{x},\mathbf{y}) &= \sum_{k=1}^{L}\mathcal{I}(x_k,y_k)\\ &= \sum_{k=1}^{L}\mathcal{E}\left\{\log_2\left|\mathbf{I}_{n_r}+\rho_{k,k}\mathbf{H}_{k,k}\mathbf{Q}_k\mathbf{H}_{k,k}^{\dagger}\cdot\left(\mathbf{I}_{n_r}+\sum_{\substack{j=1\\ j\neq k}}^{L}\rho_{k,j}\mathbf{H}_{k,j}\mathbf{Q}_j\mathbf{H}_{k,j}^{\dagger}\right)^{-1}\right|\right\}\end{aligned} \tag{4.2}$$

Hence, the capacity is the maximization of the total mutual information over all $\mathbf{Q}_k$s. This superfluous equation is encountered often and hence we write the same in a condensed form by using the interference plus noise variance term notation $\mathbf{R}_{zz,k}$, and a special function, $\Phi(\rho,\mathbf{Q},\mathbf{H}) = \log_2|\mathbf{I}_{n_r}+\rho\mathbf{H}\mathbf{Q}\mathbf{H}^{\dagger}|$

$$C = \sum_{k=1}^{L}\mathcal{E}[\Phi(\rho_{k,k},\mathbf{Q}_k,\mathbf{R}_{zz,k}^{-\frac{1}{2}}\mathbf{H}_{k,k})]. \tag{4.3}$$

Extensive proof is offered in [28] of the fact that that the sum mutual information is dependent on the SNR terms $\rho_{k,k}$ and INR terms $\rho_{k,j}$, and is concave in the limit of low interference, and convex in the case of very large interference. In the absence of channel state information at the transmitter, the solution to this optimization problem is found to be uniform power distribution among all antennas when the interference is weak in comparison to the intended signal power, and single antenna transmission in the presence of high interference and low signal power.

Figure 4.2 shows the exact simulation setup of the system, with uniformly distributed transmit nodes interfering with the link of interest because they are within the effective radius considered. For each of the receive nodes of these links (receive nodes not shown here), the interference profile can be considered to be the same as for this representative receiver.

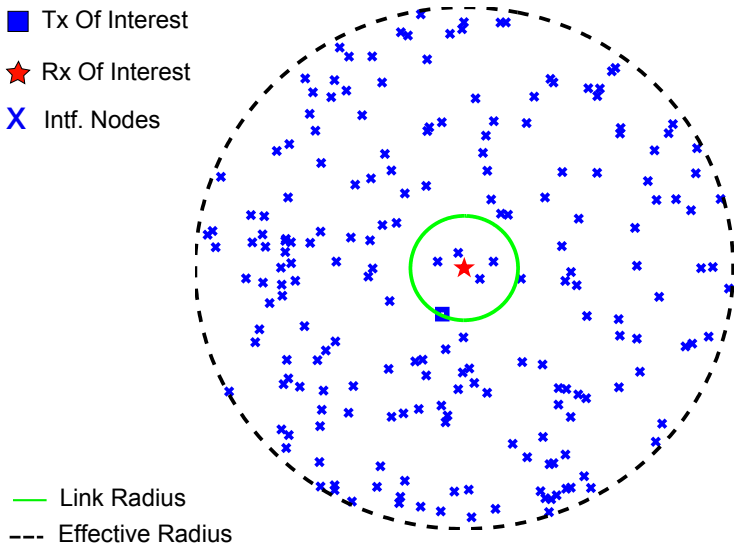

Figure 4.2: System Model for MIMO Ad Hoc Network

Our assumptions that the interference seen by one node is similar to that of any other and that there is minimal cooperation with interference transmission, and the maximization of each node pair's own channel capacity allows us to write the sum capacity to be the capacity of the representative link multiplied by the number of participating node pairs in the effective area.

$$C_{network} = L \times \mathcal{E}[\Phi(\rho_{k,k}, \mathbf{Q}_k, \mathbf{R}_{zz,k}^{-\frac{1}{2}} \mathbf{H}_{k,k})], \tag{4.4}$$

where,

$$\mathbf{R}_{zz,k} = \left(\mathbf{I}_{n_r} + \sum_{\substack{j=1 \\ j \neq k}}^{L} \rho_{k,j} \mathbf{H}_{k,j} \mathbf{Q}_k \mathbf{H}_{k,j}^{\dagger} \right) \tag{4.5}$$

Note the small change in the way $\mathbf{R}_{zz,k}$ is defined, with all the participating nodes transmitting using the same covariance matrix, and the significance of the index k is only for the channel matrices and the attenuation from each interferer.

In the absence of any channel state information, as before, the transmission is done by dividing the power equally among all the antenna. Hence, the sum capacity

of the network is now:

$$C_{UT,network} = L \times \mathcal{E}\left\{ \log_2 \left| \mathbf{I}_{n_r} + \frac{\rho_{k,k}}{n_t} \mathbf{H}_{k,k} \mathbf{H}_{k,k}^{\dagger} \cdot \left(I_{n_r} + \frac{\rho_{k,j}}{n_t} \sum_{\substack{j=1 \\ j \neq i}}^{L} \mathbf{H}_{k,j} \mathbf{H}_{k,j}^{\dagger} \right)^{-1} \right| \right\} \tag{4.6}$$

$$= L \times \mathcal{E}\left[\Phi\left(\rho_{k,k}, \frac{\rho_{k,k}}{n_t} \mathbf{I}, \mathbf{R}_{zz,k}^{-\frac{1}{2}} \mathbf{H}_{k,k} \right) \right] \tag{4.7}$$

This is ideal for transmission in low interference conditions, and [28] presents quite an involved proof of the fact that the same is not true when the interference is high. Successively simpler derivations asymptotic results for constant power from all the nodes are presented in [16] and in [17], respectively. In the upcoming simulations, these claims are verified and it is shown that in high node densities, the ideal transmission for the best sum capacity is with a single mode usage by all the participating transmitters. An asymptotic expression for the capacity is derived, a short theoretical treatment to support the simulation is presented next.

4.3 UT Sum Capacity in High Node Density Networks

The regime of an asymptotically infinite number of nodes, as considered in [17] is unrealistic and might not be the case that should be encountered in any real world situations. Also, as we will see in the simulations, the behavior of the capacity is much different and not as smooth as when all the interference power is considered to be equal per transmitter. However, it is worth looking at solely to explain some possible explanations at higher, if not asymptotic node densities, and to compare the case of UT capacity in high interference to that of the IT water filling case. For a high density of randomly distributed nodes in the effective area, due to the law of

large numbers, we can approximate the interference (only) covariance to be a spatially white Gaussian.

$$\frac{\rho}{n_t}\sum_{\substack{j=1\\ j\neq k}}^{L}\mathbf{H}_{k,j}\mathbf{Q}_j\mathbf{H}_{k,j}^{\dagger} = (L-1)\frac{\rho}{n_t}\mathbf{I}_{n_r} \tag{4.8}$$

Where we use the approximation that

$$\mathcal{E}[\mathbf{HRH}^{\dagger}] = \mathrm{tr}\{\mathbf{R}\}\mathbf{I},$$

the proof for which is given in [16]. It serves to consider this both as the ergodic capacity over all channel realizations for the node of interest or as the average of the interference of all participating node in this context.

Hence, the capacity of the channel and the network is now independent of the transmit covariance of the other transmitters. It is the number of transmitters times the channel capacity. For both equal power distribution between the antennas and lower modes transmission,

$$\begin{aligned}
\lim_{L\to\infty} C_{UT,network} &= L \times \mathcal{E}_{\mathbf{H}}\left\{\log_2\left|\mathbf{I}_{n_r} + \frac{\rho}{n_t}\times\frac{\mathbf{H}_{k,k}\mathbf{Q}_j\mathbf{H}_{k,k}^{\dagger}}{\mathbf{I}_{n_r}+(L-1)\frac{\rho}{n_t}\mathbf{I}_{n_r}}\right|\right\} && (4.9)\\
&\leq L\times\log_2\left|\mathcal{E}_{\mathbf{H}}\left\{\mathbf{I}_{n_r} + \frac{\rho}{n_t}\times\frac{\mathbf{H}_{k,k}\mathbf{Q}_j\mathbf{H}_{k,k}^{\dagger}}{\mathbf{I}_{n_r}+(L-1)\frac{\rho}{n_t}\mathbf{I}_{n_r}}\right\}\right| \\
&= L\times\log_2\left|\mathbf{I}_{n_r} + \frac{\rho}{n_t}\times\frac{\mathbf{I}_{n_r}}{\mathbf{I}_{n_r}+(L-1)\frac{\rho}{n_t}\mathbf{I}_{n_r}}\right| \\
&= Ln_r\times\log_2\left(1+\frac{\rho}{n_t}\times\frac{1}{1+(L-1)\frac{\rho}{n_t}}\right) && (4.10)\\
&\approxeq \frac{n_r}{\log_e(2)} && (4.11)
\end{aligned}$$

The last approximation is due to the property $\ln(1+x) = x$ for small x. Figure 4.3 is a plot of the Simulated and Asymptotic sum capacities for 2x2 and 4x4 MIMO Networks. We see that the asymptotic capacities are realized at node densities in the hundreds.

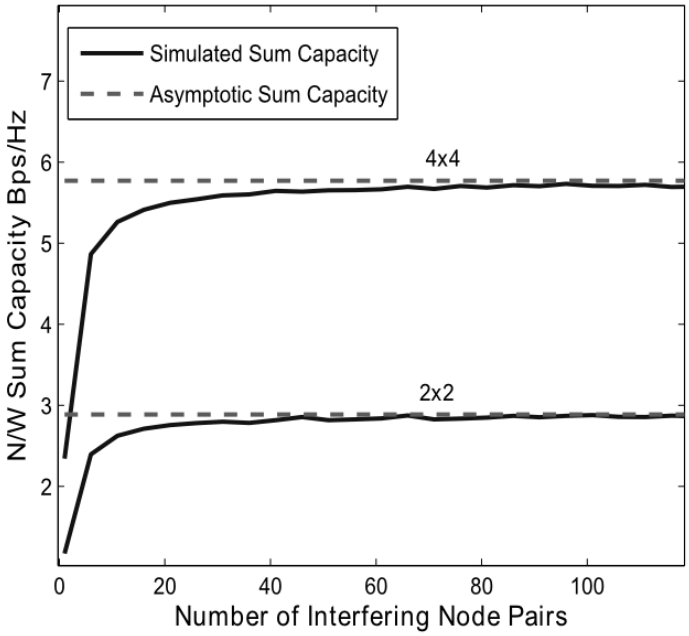

Figure 4.3: UT Network Sum Capacity for SNR=1, and different Antenna Configurations

Again, this regime is quite unrealistic, as, once the number of participating nodes increases, the capacity of each link becomes n_r/L, and the number of receive antennas has to be increased to have it in an acceptable range. The sum capacity is only independent of the transmit power because in the case of high interference, the power terms are canceled out in the numerator and the denominator. These factors are discussed in [16]. However, most importantly, in the expression (4.10), the large L in the numerator and the denominator both can be canceled because the log is in its linear region. However, if this were not the case, if there is a region where the intended signal is higher than the interference, the n_r/L term could dominate, resulting in a peak at a lower density! This is the essence of this dissertation, and in the next chapter, we show that there exists such a condition, and hope to study it in more detail.

The case of the asymptotic sum capacity in the presence of CSI is very closely related to the uninformed transmitter case, so it is presented here contiguously. However, the process of simulations for IT sum capacity is much more complex and presented soon after.

4.4 IT Sum Capacity in High Node Density Networks

The proof for optimality of single mode transmission is inherent in the derivation of the asymptotic capacity of the network. Starting with the equation (4.9), we get the optimum informed transmitter capacity:

$$\begin{aligned}\lim_{L\to\infty} C_{UT,network} &= L \times \mathcal{E}_{\mathbf{H}} \left\{ \max \log_2 \left| \mathbf{I}_{n_r} + \frac{\rho}{n_t} \times \frac{\mathbf{H}_{k,k}\mathbf{Q}_j\mathbf{H}_{k,k}^{\dagger}}{\mathbf{I}_{n_r} + (L-1)\frac{\rho}{n_t}\mathbf{I}_{n_r}} \right| \right\} \\ &= L \times \mathcal{E}_{\lambda_{W,k}} \left\{ \max \sum_{k=1}^{m} \log_2 \left(1 + \frac{\rho}{n_t} \times \frac{\lambda_{\mathbf{W},k}\varrho_k}{1 + (L-1)\frac{\rho}{n_t}} \right) \right\},\end{aligned}$$

Where the ϱ_k's (m in number) are the normalized diagonal elements of the transmit covariance, and the $\lambda_{W,k}$ are the respective eigenvalues of the channel Wishart matrix. We have dropped the index referring to the node identification because the expression now only depends on one's own transmit covariance, and this makes it much more convenient to present. Using the fact that $\log_e(1+x) \leq x$,

$$\begin{aligned}\lim_{L\to\infty} C_{UT,network} &\leq L \times \mathcal{E}_{\lambda_{W,k}} \left\{ \max \left(\frac{\rho}{n_t} \times \frac{\sum_{k=1}^{m} \lambda_{W,k}\varrho_k}{1 + (L-1)\frac{\rho}{n_t}} \right) \right\} \times \frac{1}{\log_e(2)} \\ &= \frac{L(\rho/n_t)}{1 + (L-1)(\rho/n_t)} \frac{\mathcal{E}[\lambda_{W,1}]}{\log_e(2)} \qquad (4.12)\end{aligned}$$

This is because the convex optimization

$$\max \sum_{k=1}^{m} \lambda_{W,k}\varrho_k$$

subject to

$$\sum_{k=1}^{m} \varrho_k = 1$$

when $\lambda_{W,k}$ are arranged in descending order is simply to have $\varrho_1 = 1$ and $\varrho_2 = \varrho_3, ... = \varrho_m = 0$. The mean value of the largest eigenvalue of large dimension Wishart matrices is given to be [17] $n_r + n_t + 2\sqrt{n_r n_t}$, and when $n_r = n_t$, it is simply $4m$.

More importantly, the equation is quite similar to the previous case, and we again see that the approximation works when the log is in the linear range, and the sum interference power grows linearly with the number of nodes. However, in the presence of path loss, it is not expected of the interference power to pick up so quickly, and hence a peak is possible. The per user spectral efficiency hence will have a region where it is constant or slowly decreasing as the number of participating nodes increases in the network.

4.5 Simulating IT Sum Capacity

The simulation of the network sum capacity in the case of an informed transmitter is specifically tricky.

1. For the node of interest to perform water filling, it needs to have the channel information as seen by the receiver.

2. For the network capacity to be the multiple of the link capacity, all the links must be transmitting with CSI and using water filling.

3. But for the interfering nodes to transmit using water filling, they must also know the interference covariance matrix as if the rest of the participating nodes are transmitting in a similar manner.

4. In the steady state, all the transmissions in the network are done with CSI but for any of them to start transmission, all the others must already be transmitting!

5. The problem is figuring out a turnkey iterative starting scenario, and repeating it until the equilibrium state is reached.

The method used in this dissertation is partly similar to the Sum Capacity method used with the uninformed transmission, but with adjustments made repeatedly until there is no change seen in the system behavior. We can then assume that the network capacity is the number of participants times the channel capacity. Figure 4.4 is a flowchart that summarizes the iterative process.

A good way to evaluate the system state is to plot the eigenvalue spectrum of the transmit covariance matrix and see how it changes after each iteration. Figure 5.3 shows the eigenvalue spectrum after the first 8 iterations for 4x4 and 8x8 MIMO

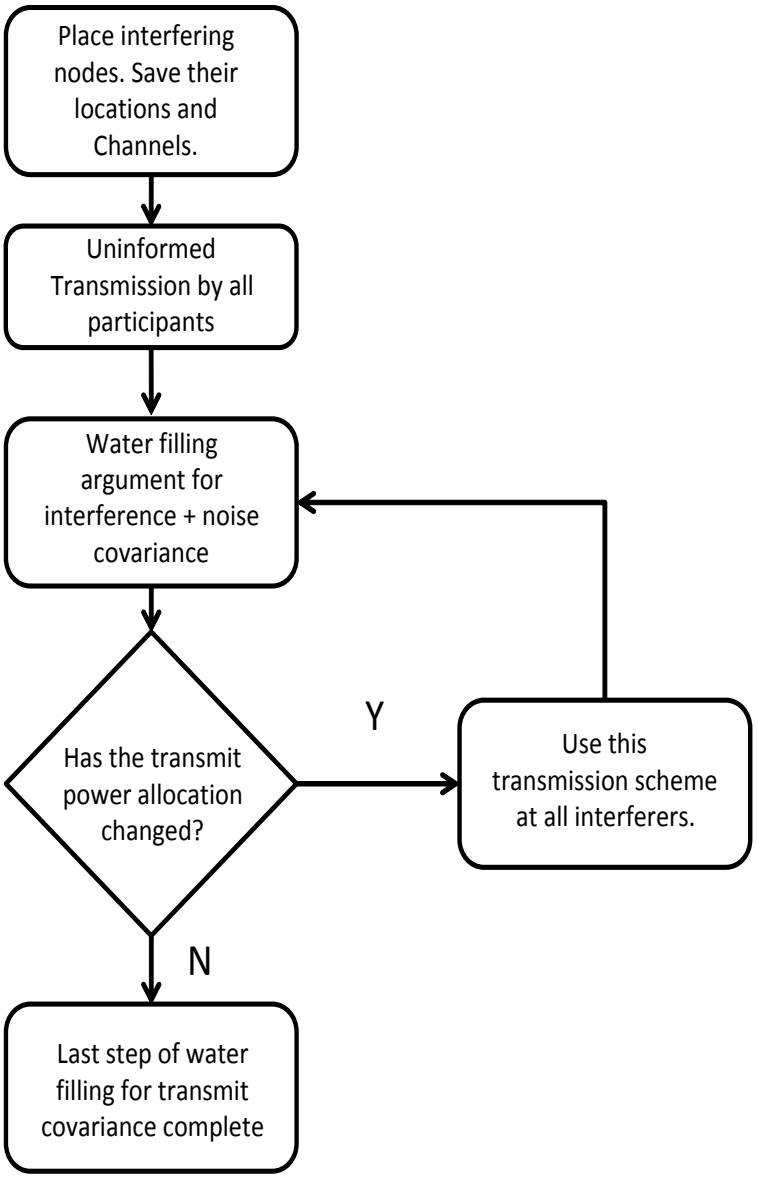

Figure 4.4: IT-MIMO Network Simulation Setup

links. Further discussion is deferred until we reach that part of the document. It suffices to know that fewer than 8 iterations prove to be enough to achieve the total sum capacity condition.

4.6 Interference Rank of a MIMO Network

In the simulations that follow, we evaluate the Network Spectral Efficiency as the network accrues more and more participants. Some common parameters to intuitively vary and check the Network Spectral Efficiency would be simply the number of participating node pairs (precisely, the number of transmitters) or the density of transmit nodes. When the network has few participants, the addition of even a single interferer makes a big difference, motivating us to use the node-pair number as the metric. Liu J. et al. present the exact numerical solution for networks with around ten participants [15]. For a bigger network, it would be optimum to consider the node density as it would be much more robust to compare across networks of different areas. Further, a metric that would take into consideration both the strength of the transmission of interest, and the strength of the least bothersome interference would provide more intuition. Interference Rank is one such metric that is both simple and more intuitive at the same time. Interference rank is the ratio of the interferers that may be closer to the representative receiver than the corresponding transmitter, and the total number of participating transmit nodes in the representative network. It means that some interferers are more important than others. We can obtain the node density by dividing the interference rank by the link area and hence there need not necessarily be even one interferer between the Tx and Rx of interest to have a non-zero Interference Rank. i.e., when there is just one interfering node placed far from the receiver of interest, the interference rank is not zero, but is a small number that assigns some importance to this sole interferer. In [17], we see that with a constant power assumption, the Network Spectral Efficiency approaches the large L conditions with as few as 16 and 50 interferers for 4×4 and 8×8 MIMO systems respectively. For massively large networks with areas spanning Kilometers, interference rank is a

better metric, also because with path loss and random placement of the nodes, not all interferers have considerable impact.

In the next chapter, the simulations performed are presented along with the simulation parameters and the results are analyzed.

Chapter 5

SIMULATION AND RESULTS

5.1 Simulation Setup

The simulation set up is as shown in Figure 4.2. The effective area of the network is decided by the interference level that we allow to be a part of the interference profile. The link radius, on the other hand is dependent on the SNR we assume to be the operating condition. This is a level that we choose, but yet again, it is important to note that using the interference rank can still preserve the generality of the results and will make it valid for comparison with other systems in terms of behavior, although the values of the spectral efficiency might not be exactly the same. For the channel model, as suggested before, we will use a Rayleigh fading quasi-static channel. For the path loss, the parameters are arrived at empirically, by assuming a bandwidth of 10MHz, and an snr of 10dB at around 100 m for a transmit power of 200 mW, and we work our way backwards to get a coefficient of path loss to be approximately -40dB. A path loss exponent of 3.8 was chosen to model a large urban-area setting. This gives a link radius of 57.5 m and an outer radius of 480 m for a cut-off interference level of -15dB. An inner radius for the interference level of -10dB is used to evaluate the spectral efficiency to account for a certain level of soft cut-off. The most revelatory plots are the ones for the IT and UT Network Spectral Efficiency across interference ranks, as presented in this chapter. Also included is the per-user spectral efficiency, which is suffering from the addition of interferers as expected.

5.2 Uninformed MIMO Network Area Spectral Efficiency Density

The per-user uninformed-transmitter MIMO spectral efficiency is shown in the figure 5.1. We see that at low densities, employing all the available antennas is optimal, but the spectral efficiency of the network is not the optimal as one might expect, and will be obvious in the next result.

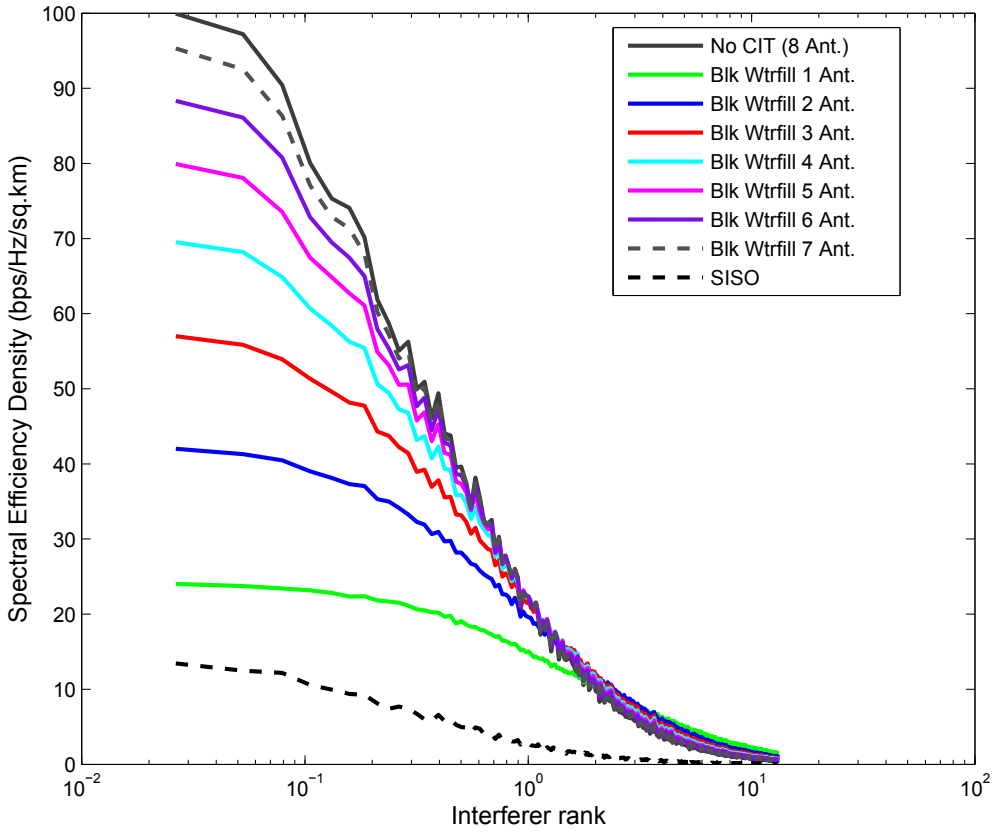

Figure 5.1: Per User Spectral Efficiency Density of the Uninformed Transmitter 8x8 MIMO Case

We see that as the number of antennas is successively reduced, the per user spectral efficiency density comes down too, at lower interference ranks. In [28], it is shown that

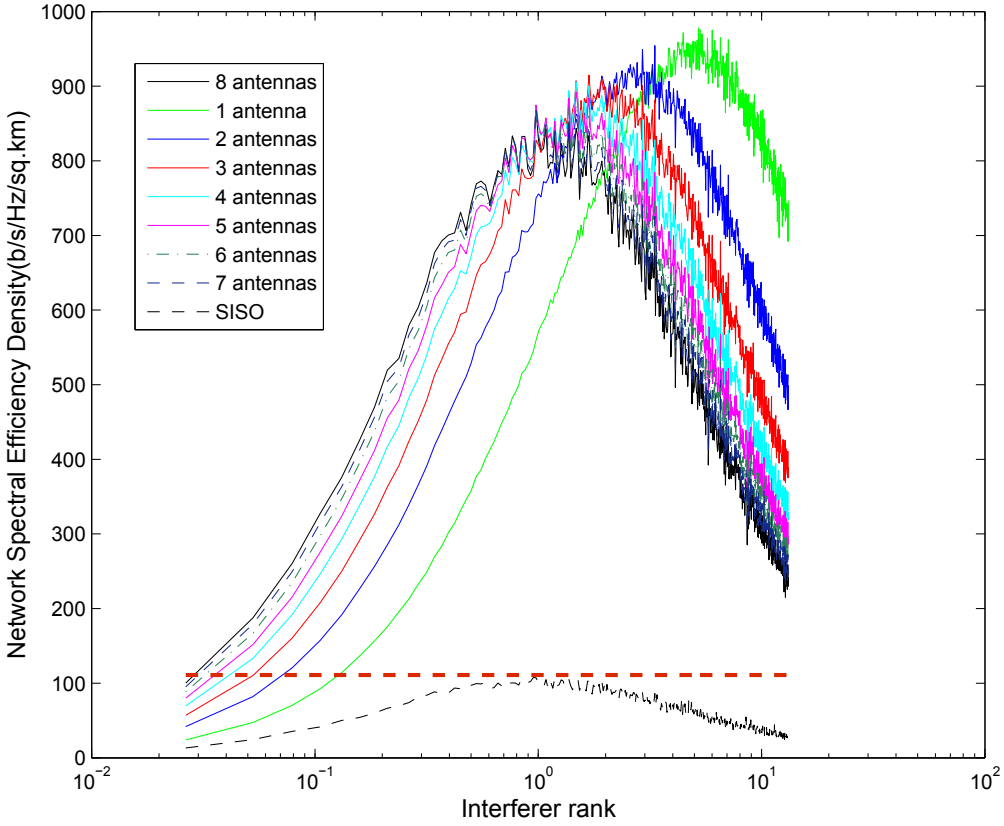

Figure 5.2: Network Spectral Efficiency Density of the Uninformed-transmitter 8x8 MIMO Case

in the low interference region, a concave optimization problem of optimal capacity results in the solution which suggests equal power distribution among all the available transmit antennas. Similarly, in high interference, the chosen power distribution scheme for a convex optimization problem is that of putting all the power into a single antenna. We see these effects in the figure, but the same effects are magnified in the network spectral efficiency, as seen next.

Now we see the network spectral efficiency density when the transmission is done blindly by dividing the power equally among the antennas by both the transmitter

of interest and all the interferers (figure 5.2). With fewer antennas employed, the power is divided only among those many antennas. It is not important which antennas are used, but only how many. The most important result to note from figure 5.2 is that there exists a particular interference rank at which the network spectral efficiency density peaks, for each of the mode usage scenarios. Second, the single transmission mode case is seen to dominate the rest at the higher densities. This is consistent with the theorized treatment from sections 4.3 and 4.4. As the interference rank gets higher, the best performing transmission decision comes out to be choosing the lower number of antennas. We can hence divide the interference rank space into regions where a certain scheme is the best. The dotted line in red represents the spectral efficiency of a single 8x8 MIMO link if it were operating in a MAC arrangement such that any interference over -15dB was taken as a busy channel and either itself or the interferer would not be able to operate (it is not the scheduled average throughput, which would be half as much, but the momentary spectral efficiency). The improvement is very marked.

5.3 Informed MIMO Network Area Spectral Efficiency Density

We use the water filling solution proposed in section 4.5 and represented in the flowchart of figure 4.4 for the IT MIMO Spectral Efficiency case. The interference plus noise covariance matrix might never truly become constant, and we can use a particular number of iterations, in our case 10, after which the changes in the transmit covariance are tolerable, and we can assume that everyone uses the same transmission scheme. One such example is shown in Figure 5.3, for the case of 5 transmit modes and interference rank 6. We see the eigenvalue distribution of this case for the first 8 iterations, and it is obvious that the change in the values is very drastic in the first three iterations, after which the values are lumped together. This convergence

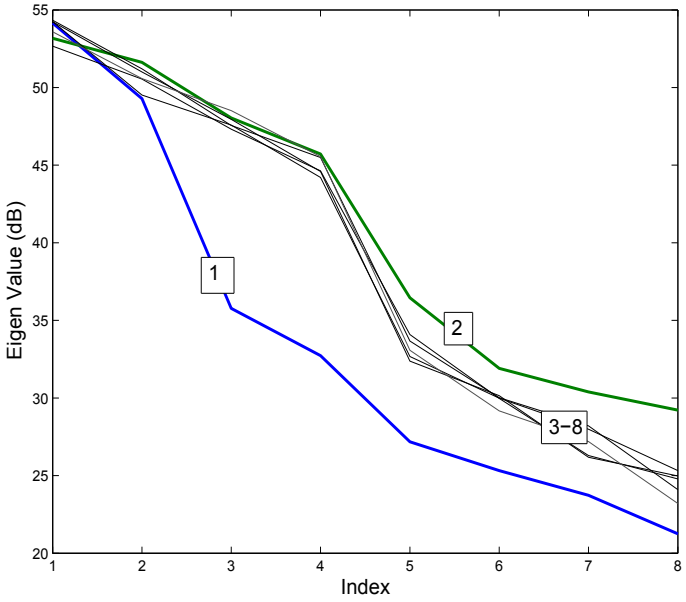

Figure 5.3: Eigenvalue Distribution of the Transmit Covariance While Using 5 Modes at an Interference Rank of 6.

might be even quicker if we assume all participants to have the water-filling transmit covariance similar to that of the link of interest to begin with, but as far as the simulation is concerned, the number of overall water-filling iterations would remain the same (it is the question of what the assumption is in the first step of our flow chart).

The per-user IT-MIMO Spectral Efficiency Density is shown in the Figure 5.4. We see some improvement in the peak per-user spectral efficiency which is simply the interference-dodging capability of the water filling algorithm. As in the case of IT MIMO, the spectral efficiency drops off In Figure 5.5, we see the Network Spectral Efficiency density of the IT-MIMO 8x8 case. A few important observations are as follows:

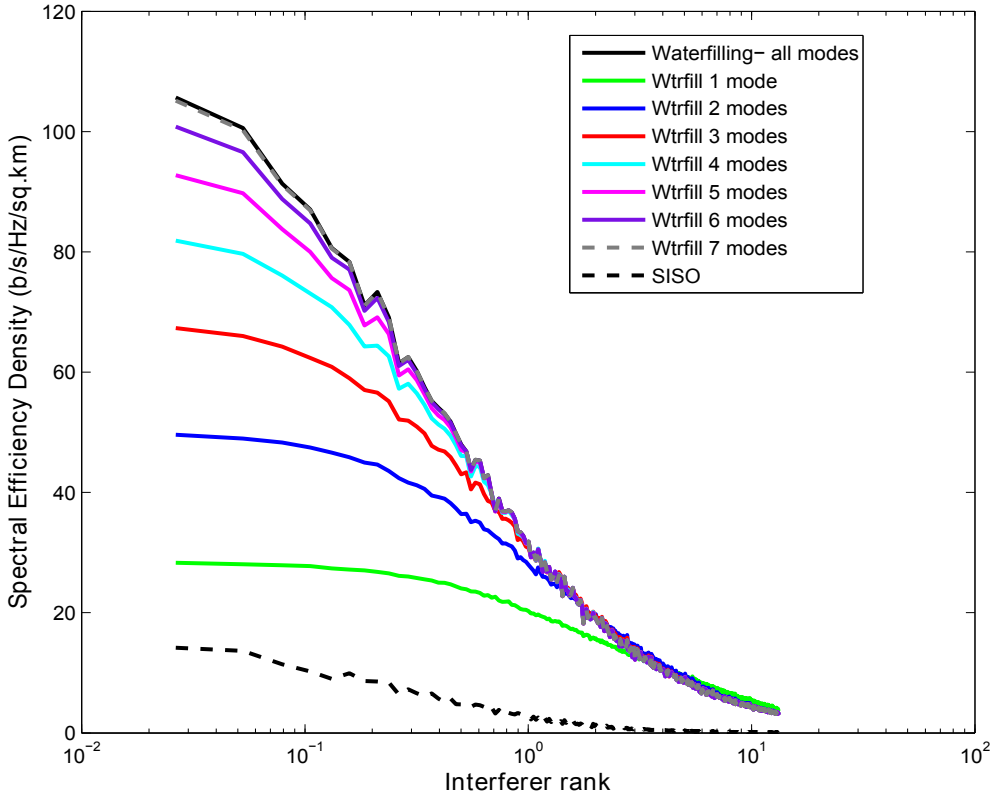

Figure 5.4: Per- user IT-MIMO Spectral Efficiency Density for 8x8 MIMO

1. We see a marked increase in the peak spectral efficiency of the network in the IT-MIMO case over the UT-MIMO case. This is expected of the single link case, as the water filling transmission makes the IT-MIMO a more intelligent case, responding to the interference or noise in the channel, and hence it is not surprising (but still remarkable) that we see the same effect for the whole network. The red dotted line is the 8x8 IT MIMO spectral efficiency if all interference was restricted.

2. Again, there is a peak spectral efficiency density at some Interference Rank for each of the mode usage cases and at very high interference rank, the single-mode

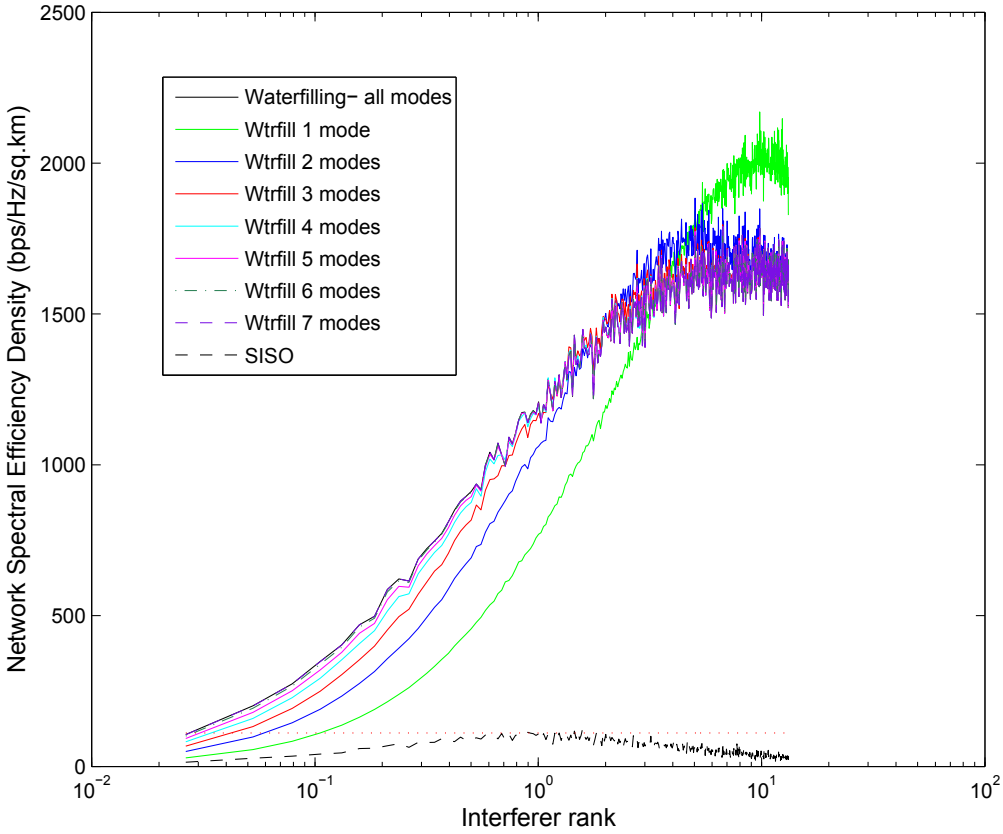

Figure 5.5: Network Spectral Efficiency Density for the IT-MIMO 8x8 case

transmission triumphs, as was theorized in Section 4.3. At very low interference rank, using all the available modes is the best option.

3. After a certain interference rank, three or higher employed modes have the same spectral efficiency density, and this is explained next. We see that the curves for these cases are all fused together, while the single mode and the two-mode cases remain separate.

To have a closer look at the performance of the IT-MIMO cases, a plot of the network area spectral efficiency density is presented again in Figure 5.6. Below it, a color map matrix corresponding to the particular interference rank is shown. Each cell in this

matrix is the average number of modes that was chosen for transmission during the simulation using water filling algorithm. The vertical axis is the number of modes that the simulation allows the transmitters to use. For example, row 1, column 1 represents the simulation in which we allowed the water filling algorithm to use all 8 modes, and the case is of 0.1 interference rank. The color shows that is uses close to 8 and definitely more than 7 modes on an average.

If the interference in a particular spatial sub-channel is particularly high, we know that the water filling algorithm refrains from putting any power into this mode. As the interference increases, even though there is no constraint on how many modes the algorithm can choose to use applied by the simulation, the higher mode-cases still choose to pour the power into fewer modes, and as the interference rank increases, we see that if we take a look at the matrix vertically, the 3 or higher mode-cases are of the same color (i.e., they use the same number of modes on average). However, by principle, the water filling algorithm is still a selfish algorithm, and in the presence of only link-CSI, the allocation of power is done so as to maximize the capacity of the link of interest. In the case of 1 and 2-mode simulations, we are restricting the transmission further to fewer modes (the total transmit power is still the same) and the Network spectral efficiency is seen to increase, while, as seen in the last two rows of the matrix, the number of modes actually used on an average are different from the other cases.

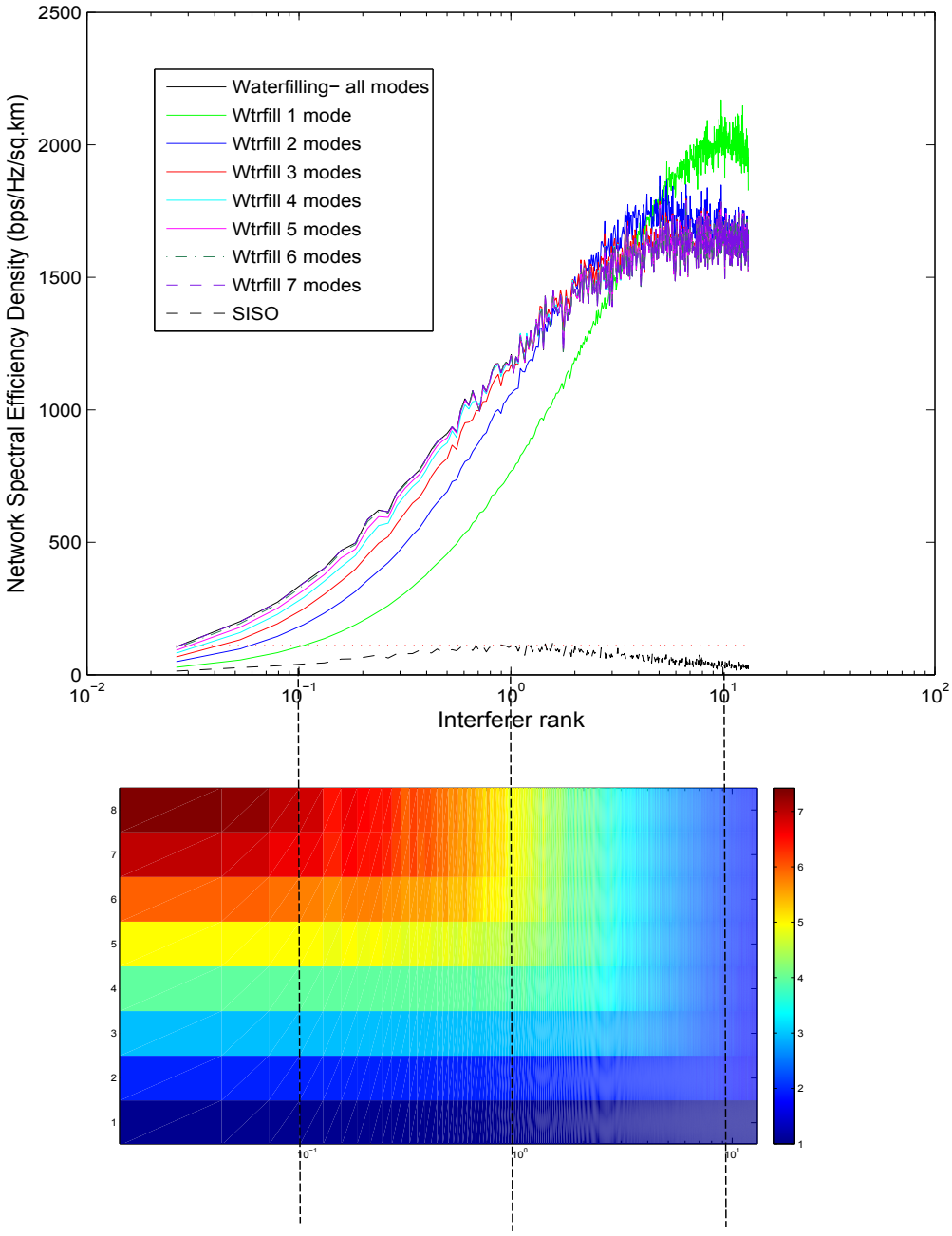

Figure 5.6: Average Number of Modes Used in the Simulation for Each of the Mode-usage Cases

Chapter 6

CONCLUSION AND FUTURE WORK

6.1 Conclusion

1. The Network Area Spectral Efficiency of highly populated MIMO ad hoc networks was presented. A method to simulate the same for Informed and Uninformed Transmitter cases was proposed.

2. A metric against which to compare the network spectral efficiency density across systems, known as Interference Rank (section 4.6), was put forward.

3. The results show that there exists a certain interference rank at which the NASE peaks for any particular transmission scheme. This means that spatial clustering limits performance and motivates the study of density controlling MAC.

4. Yet another utile result is the matrix plot of the number of modes used under a scheme where the more altruistic decision is proving beneficial to the network as a whole, which is a 'Statistical MAC' condition where the media access is self-restricted based on the deployed conditions of the network. When the link rank space is divided into regions where a particular scheme has the highest spectral efficiency for the network, this can be the imposed access control restriction, in addition to the MAC layer.

5. Previously theorized result that using one transmit stream is optimal at very high node density situations was verified through simulation.

6.2 Possible Future Work

An immediate next step forward is to find ways to use the obtained plots in optimizing the spectral efficiency of the network. This may be by employing interference rank as a MAC metric to design access control protocols, or by identifying the number of modes to be used as the density of the system changes to get the best throughput. We have to control the limiting effect of spatial clustering with a density controlling MAC. Similarly, a further level of interference rejection of far away interferers in the simulation is to emulate the total network with fewer interferers that matter more using the interference rank, i.e., to approach the interference profile of the whole network with only the rank-participating interferers. This means that the behavior of smaller portions of the network consisting of these interferers when using a particular number of modes is similar to the behavior of the entire network doing the same. An ergodic approximation of the network area spectral efficiency can be made using the channel model parameters to obtain a rough curve that closely approaches the

Now that the constant power interference and simplified path loss model interference cases have been considered, it might also prove worthwhile to explore more realistic physical system assumptions and propagation models, as a practical step ahead.

REFERENCES

[1] A.J. Paulraj, D.A. Gore, R.U. Nabar, and H. Bolcskei. An overview of MIMO communications - a key to gigabit wireless. *Proceedings of the IEEE*, 92(2):198–218, Feb 2004.

[2] Daniel W. Bliss and Siddhartan Govindasamy. *Adaptive Wireless Communications: MIMO Channels and Networks*. Cambridge University Press, 2013.

[3] Daniel W. Bliss, Keith W. Forsythe, and Amanda M. Chan. MIMO wireless communication. *Lincoln Laboratory Journal*, 15(1):97–126, 2005.

[4] Steven Cherry. Edholm's law of bandwidth - telecommunications data rates are as predictable as moore's law. Jul 2004.

[5] D. Gesbert, M. Shafi, Da shan Shiu, P.J. Smith, and A. Naguib. From theory to practice: an overview of MIMO space-time coded wireless systems. *Selected Areas in Communications, IEEE Journal on*, 21(3):281–302, Apr 2003.

[6] Rohde and Schwarz. Introduction to MIMO, application note 1ma1420e. Jul 2009.

[7] W.P. Siriwongpairat, W. Su, M. Olfat, and K.J.R. Liu. Multiband-ofdm MIMO coding framework for uwb communication systems. *Signal Processing, IEEE Transactions on*, 54(1):214–224, Jan 2006.

[8] F. Khalid and J. Speidel. Advances in MIMO techniques for mobile communications, a survey. 2010.

[9] Emre Telatar. Capacity of multi-antenna gaussian channels. *European transactions on telecommunications*, 10(6):585–595, 1999.

[10] N. Chiurtu, B. Rimoldi, and I.E. Telatar. On the capacity of multi-antenna gaussian channels. In *Information Theory, 2001. Proceedings. 2001 IEEE International Symposium on*, pages 53–, 2001.

[11] N. Chiurtu, B. Rimoldi, and I.E. Telatar. Dense multiple antenna systems. In *Information Theory Workshop, 2001. Proceedings. 2001 IEEE*, pages 108–109, 2001.

[12] N. Chiurtu, B. Rimoldi, I.E. Telatar, and V. Pauli. Impact of correlation and coupling on the capacity of MIMO systems. In *Signal Processing and Information Technology, 2003. ISSPIT 2003. Proceedings of the 3rd IEEE International Symposium on*, pages 154–157, Dec 2003.

[13] Daniel W. Bliss, Keith W. Forsythe, Alfred O. Hero, and Ali F. Yegulalp. Environmental issues for MIMO capacity. *Signal Processing, IEEE Transactions on*, 50(9):2128–2142, 2002.

[14] A. Goldsmith, S.A. Jafar, N. Jindal, and S. Vishwanath. Capacity limits of MIMO channels. *Selected Areas in Communications, IEEE Journal on*, 21(5):684–702, June 2003.

[15] Jia Liu, Y.T. Hou, Yi Shi, H.D. Sherali, and S. Kompella. On the capacity of multiuser MIMO networks with interference. *Wireless Communications, IEEE Transactions on*, 7(2):488–494, February 2008.

[16] Biao Chen and M.J. Gans. MIMO communications in ad hoc networks. *Signal Processing, IEEE Transactions on*, 54(7):2773–2783, July 2006.

[17] Z. Motamedi and M.R. Soleymani. Asymptotic spectral efficiency of MIMO ad hoc networks. *Signal Processing, IEEE Transactions on*, 58(1):462–466, Jan 2010.

[18] Yi Song and Steven D. Blostein. MIMO channel capacity in co-channel interference.

[19] D.W. Bliss, K.W. Forsythe, and A.F. Yegulalp. MIMO communication capacity using infinite dimension random matrix eigenvalue distributions. In *Signals, Systems and Computers, 2001. Conference Record of the Thirty-Fifth Asilomar Conference on*, volume 2, pages 969–974 vol.2, Nov 2001.

[20] Siddhartan Govindasamy, Daniel W. Bliss, and David H. Staelin. Asymptotic spectral efficiency of multi-antenna links in wireless networks with limited tx csi. *IEEE Transactions on Information Theory*, 58(8):5375–5387, 2012.

[21] O. Leveque and I.E. Telatar. Information-theoretic upper bounds on the capacity of large extended ad hoc wireless networks. *Information Theory, IEEE Transactions on*, 51(3):858–865, March 2005.

[22] Ming Kang and M.-S. Alouini. Impact of correlation on the capacity of MIMO channels. In *Communications, 2003. ICC '03. IEEE International Conference on*, volume 4, pages 2623–2627 vol.4, May 2003.

[23] Marco Chiani, Moe Z. Win, and Alberto Zanella. On the capacity of spatially correlated MIMO rayleigh-fading channels. *Information Theory, IEEE Transactions on*, 49(10):2363–2371, 2003.

[24] Ming Kang and M.-S. Alouini. Capacity of MIMO rician channels. *Wireless Communications, IEEE Transactions on*, 5(1):112–122, Jan 2006.

[25] Andrea Goldsmith. *Wireless Communications*. Cambridge University Press, Aug 2005.

[26] Bengt Holter. On the capacity of the MIMO channel: A tutorial introduction. *Proc. IEEE Norwegian Symposium on Signal Processing*, 2001.

[27] C. Oestges and B. Clerckx. *MIMO Wireless Communications: From Real-World Propagation to Space-Time Code Design*. Elsevier Science, 2010.

[28] R.S. Blum. MIMO capacity with interference. *Selected Areas in Communications, IEEE Journal on*, 21(5):793–801, June 2003.

[29] M.-A. Khalighi, J. Brossier, G.V. Jourdain, and K. Raoof. Water filling capacity of rayleigh MIMO channels. In *Personal, Indoor and Mobile Radio Communications, 2001 12th IEEE International Symposium on*, volume 1, pages A–155–A–158 vol.1, Sep 2001.

[30] Bruce F. McGuffin and Daniel W. Bliss. Mobile MIMO capacity in network interference: Informed and uninformed transmitters. In *MILITARY COMMUNICATIONS CONFERENCE, 2012-MILCOM 2012*, pages 1–6. IEEE, 2012.

[31] Daniel W. Bliss and Keith W. Forsythe. Information theoretic comparison of MIMO wireless communication receivers in the presence of interference. In *Signals, Systems and Computers, 2004. Conference Record of the Thirty-Eighth Asilomar Conference on*, volume 1, pages 866–870. IEEE, 2004.

[32] M. Fatih Demirkol and Mary Ann Ingram. Stream control in networks with interfering MIMO links. In *Wireless Communications and Networking, 2003. WCNC 2003. 2003 IEEE*, volume 1, pages 343–348. IEEE, 2003.